DISSERTATIONES
SCIENTIAE
MATERIALIS
UNIVERSITATIS
TARTUENSIS
32

EVGENII STRUGOVSHCHIKOV

First-principles studies on rare-earth metal-hydride-based smart materials

DISSERTATIONES SCIENTIAE MATERIALIS UNIVERSITATIS TARTUENSIS
32

EVGENII STRUGOVSHCHIKOV

First-principles studies on rare-earth metal-hydride-based smart materials

UNIVERSITY OF TARTU
Press

Institute of Physics, Faculty of Science and Technology, University of Tartu, Estonia.

Dissertation has been accepted for the commencement of the degree of Doctor of Philosophy (PhD) in Material Science on September 7th, 2021 by the Council of the Institute of Physics, University of Tartu.

Supervisor

Dr. Aleksandr Pishtshev,
Research Fellow in Solid State Theory,
Institute of Physics, University of Tartu,
Tartu, Estonia.

Prof. Dr. Smagul Karazhanov,
Senior Researcher,
Department for Solar Energy, Institute for Energy Technology,
Kjeller, Norway.

Opponents

Prof. Dr. Peter Kratzer,
Faculty of Physics, University of Duisburg-Essen,
D-47048 Duisburg, Germany

Dr.habil.phys., Prof. Juris Purans
Institute of Solid State Physics, University of Latvia
8 Kengaraga St., LV-1063 Riga, Latvia

The public defense will take place on October 21st, 2021 at 12:15 in the University of Tartu, Estonia.

The publication of this dissertation was financed by the Institute of Physics, University of Tartu.

ISSN 2228-0928
ISBN 978-9949-03-711-7 (print)
ISBN 978-9949-03-712-4 (PDF)

University of Tartu Press
http://www.tyk.ee/

CONTENTS

LIST OF ABBREVIATIONS

REM:	Rare-earth metals
CFS:	Crystal field splitting
VBM:	Valence band maximum
CBM:	Conduction band minimum
DOS:	Density of states
XRD:	Xray-diffraction
GI-XRD:	Grazing Incidence XRD
ToF-E ERDA:	Time-of-Flight/Energy co-incidence Elastic Recoil Detection Analysis
XPS:	X-ray photoelectron spectroscopy
T:	Transmittance (optical)
R:	Reflectance (optical)
UV:	Ultraviolet
LED:	Light-emitting diode
DFT:	Density functional theory
O_h:	Octahedral group
VASP:	Vienna Ab-initio Simulation Package
HF:	Hartree-Fock approximation
GGA:	Generalized gradient approximation
HSE:	Heyd–Scuseria–Ernzerhof exchange–correlation functional
PAW:	Projector Augmented Wave-functions
PVDF:	Polyvinylidene fluoride
NLO:	Nonlinear optics

LIST OF ORIGINAL PUBLICATIONS

Publications included in the thesis

[I] Aleksandr Pishtshev, **Evgenii Strugovshchikov**, and Smagul Karazhanov. "Conceptual Design of Yttrium Oxyhydrides: Phase Diagram, Structure, and Properties". In: *Cryst. Growth Des.* 19.5 (2019), pp. 2574–2582. DOI: https://doi.org/10.1021/acs.cgd.8b01596.

[II] Aleksandr Pishtshev and **Evgenii Strugovshchikov**. "Computational prediction of Ferro- and Piezoelectricity in Lead-free Oxyhydrides Ln_2H_4O (Ln = Y, La)". In: *Adv. Theory Simul.* 2.12 (2019), p. 1900144. DOI: https://doi.org/10.1002/adts.201900144.

[III] Aleksandr Pishtshev, **Evgenii Strugovshchikov**, and Smagul Karazhanov. "On prediction of a novel chiral material $Y_2H_3O(OH)$: A hydroxyhydride holding hydridic and protonic hydrogens". In: *Materials* 13.4 (2020), p. 994. DOI: https://doi.org/10.3390/ma13040994.

[IV] Elbruz Murat Baba, Jose Montero, **Evgenii Strugovshchikov**, Esra Özkan Zayim, and Smagul Karazhanov. "Light-induced breathing in photochromic yttrium oxyhydrides". In: *Phys. Rev. Mater.* 4.2 (2020), p. 025201. DOI: https://doi.org/10.1103/PhysRevMaterials.4.025201.

[V] **Evgenii Strugovshchikov** and Aleksandr Pishtshev. "Exploring The Anion Chemical Space of $Ln_2OF_{2-x}Cl_xH_2$ (Ln=Y,La,Gd): A Model of Electroelastic Material with High Mechanical Sensitivity and Energy Harvesting". In: *Mater. Horiz.* 8.2 (2021), pp. 577–588. DOI: https://doi.org/10.1039/D0MH01524E.

[VI] **Evgenii Strugovshchikov**, Aleksandr Pishtshev, and Smagul Karazhanov. "Orthogonal chemistry in the design of rare-earth metal oxyhydrides". In: *Pure Appl. Chem.* -.- (2021), pp. -. DOI: https://doi.org/10.1515/pac-2021-0207.

[VII] **Evgenii Strugovshchikov**, Aleksandr Pishtshev, and Smagul Karazhanov. "Theoretical design of effective multilayer optical coatings using oxyhydride thin films". In: *Phys. Status Solidi B* -.- (2021), pp. -. DOI: https://doi.org/10.1002/pssb.202100179.

Author's contribution:

In the **Paper I** the author's part was performing the first-principles calculations as well as artwork, data analysis, discussions, review and editing, and approval of the manuscript.

In the **Paper II** the author's part was the planning and performing the theoretical research as well as conceptualization, artwork, data analysis, discussions, review and editing, and approval of the manuscript.

In the **Paper III** the author's part was the planning and performing the theoretical computations as well as conceptualization, artwork, data analysis, discussions, review and editing, and approval of the manuscript.

In the **Paper IV** the author's part was performing the first-principles calculations as well as the data analysis and artwork.

In the **Paper V** the author's part was the planning and performing the theoretical research as well as conceptualization, artwork, data analysis, discussions, review and editing, and approval of the manuscript.

In the **Paper VI** the author's part was the planning and performing the theoretical research as well as conceptualization, artwork, data analysis, discussions, review and editing, and approval of the manuscript.

In the **Paper VII** the author's part was the planning and performing the theoretical research as well as conceptualization, artwork, data analysis, discussions, review and editing, and approval of the manuscript.

Approval of results

Results were discussed at the 8th World Congress on Nanotechnology and Materials Science (April 24–26, 2019, Amsterdam, Netherlands), the International Congress on Advanced Materials Sciences and Engineering (AMSE-Japan) (July 22–24, 2019, Osaka, Japan), the International Conference on Chemistry and Analytical Techniques (November 14–15, 2019, San Francisco, USA), and at the N.I.C.E. – 2020 International Conference (October 12–14, 2020, Nice, France). Results were also reported at the Doctor school conferences "Functional materials and technologies" in 2018, 2019, 2020 and 2021 (Tartu and Tallinn, Estonia) and at the student physics seminars (Tartu, Estonia).

Publications not included in the thesis

[VIII] P. V. Borisyuk, E. V. Chubunova, Yu. Yu. Lebedinskii, E. V. Tkalya, O. S. Vasilyev, V. P. Yakovlev, **E. Strugovshchikov**, D. Mamedov, A. Pishtshev, and S. Zh. Karazhanov. "Experimental studies of thorium ion implantation from pulse laser plasma into thin silicon oxide layers". In: *Laser Physics Letters* 15.5 (2018), p. 056101. DOI: https://doi.org/10.1088/1612-202x/aaacf8.

[IX] E.A. Vagapova, **E. Strugovshchikov**, E.O. Orlovskaya, A.S. Vanetsev, L. Dolgov, L. Puust, L.D. Iskhakova, U. Maeorg, A. Pishtshev, and Yu.V. Orlovskii. "Combined spectroscopic and DFT studies of local defect structures in beta-tricalcium phosphate doped with Nd(III)". In: *Journal of Alloys and Compounds* 15.5 (2021), p. 160305. DOI: https://doi.org/10.1016/j.jallcom.2021.160305.

1. INTRODUCTION

The implementation of new multi-anion materials can enable a wide range of useful functionalities that will be needed in modern technological applications, primarily in high-performance optical and electronic devices [11, 12]. The simplest compositions of these materials comprise two-anion systems, which form such well-known families of ternary compounds as oxyhydroxides [13, 14, 15], oxynitrides [16, 17, 18] oxyfluorides [19, 20, 21, 22], and oxyhydrides [23, 24]. Chemical engineering of rare earth oxyhydrides was initiated more than 10 years ago to improve a number of key properties of metal hydrides [25, 26, 27]. It was found that the introduction of oxygen into the hydride structure not only rearranges the stoichiometry due to the flexible stabilization of hydrogen and oxygen positions in the host lattice, but also greatly expands the chemical potential of the modified metal-hydride system due to the direct addition of oxygen [23, 24, 28, 29, 30, 31]. The most important feature of stabilization of the oxyhydride compound is that in the condensed state two or more anions (such as O^{2-} and H^{-}) located near the metal cation are balanced by coordinated sharing of the common crystal space [11, 12, 30]. This opens up great potential for further functionalization of these materials, giving direct control over optical and electronic responses [32, 33, 34]. In this aspect, the recent experimental discovery that rare-earth hydrides, when partially oxidized, can exhibit photochromic properties under the exposure to visible or ultraviolet light [25, 26, 27, 35] is fundamentally important. This work was continued by several research groups in order to understand what new effects might arise due to the mutual interplay between the introduced oxygen and the crystal lattice of the hydride compound [36, 37, 38, 39, 40]. The focus of numerous experimental works was primarily on the electronic and optical properties of these new materials. In particular, it is worth noting the reports of the discovery of persistent photoconductivity and reversible color change under exposure to light [25, 41], as well as the lattice contraction effect [42] and the possibility of band gap engineering [43]. Several characteristics of the electronic structure were determined by UV-vis spectrophotometry [44] and optical ellipsometry [45]. In technological aspect, it should also be noted that the significant advantage of photochromic devices based on $Y-H-O$ systems is evidenced by the fact that the light-induced drop in transmittance occurs uniformly at all wavelengths of sunlight. Whereas, in contrast to this case, in known oxide-based photochromic devices such as WO_3, illumination with ultraviolet or blue light leads to the formation of mid-gap states that block visible light. Moreover, inorganic materials are more durable than x-chromatic devices based on polymers [46].

The results of the previous investigations, as well as Pishtshev and Karazhanov's theoretical work [31], inspired the present study. Our goal was to significantly increase our knowledge of the physical and chemical behavior of oxygen in rare-earth metal hydrides. In particular, the question of how much oxygen the ensemble of interacting particles is ready to trap, accommodate, and order has remained

entirely unclear until now. However, this amount is the most important parameter to control the stability and material properties of a given system. Moreover, no explanation has yet been obtained for the experimental fact that changing the ratio of oxygen to hydrogen can significantly affect the elastic, electronic, and optical properties of the oxyhydride system. Thus, a theoretical understanding of the chemical addition of oxygen and its functional role in the properties of solid oxyhydrides is very important for the development of new materials with unique characteristics. Another reason for the deep study of oxyhydrides is the expectation that materials derived from them will be very promising for creating new elements, films, and devices that can be used in solid-state optoelectronics, photochromic and sensor technologies, as well as in hydrogen storage systems. Our research strategy is based not only on a thorough treatment of the results of the first-principles calculations. This is because the typical requirements for computing material characteristics are usually based on a number of costly numerical procedures and intuitive assumptions. In our work, we follow a more comprehensive approach, combining a systematic analysis of the computational results with the group-theoretical methods of mathematical crystallography. This allows us to simulate material properties through the theoretical design of various crystal models. The studies become more profound and trustworthy because this approach allows simulating and predicting the composition-structure-property relationships at the atomic level.

The main aim of the present PhD thesis is the rare-earth metal oxyhydrides Y−H−O, La−H−O and Gd−H−O which will be studied by using a combination of the theoretical and computational strategies. We will examine in detail the structural, electronic, vibrational, and optical properties of these materials, analyze features of chemical bonding and structure-property relationships, and perform theoretical modeling of oxidation processes and crystal assemblies. To successfully implement the main aim, the following secondary objectives have been under the research focus:

1) schemes of rational design of oxyhydride systems in terms of first-principle modeling of partial oxidation of metal hydrides, analysis of chemical bonding and stability of different lattice configurations;

2)prediction of the phase diagram, crystal chemistry and physics of the most attractive oxyhydride models;

3) computational characterization of material properties of the oxyhydride systems;

4) establishing structure-property relationships in oxyhydride systems, understanding the key role of oxygen in the control of electronic and optical properties.

5) model design of oxyhydride films with oxygen-controlled optical properties.

The results of the planned studies are expected to expand the knowledge base on the material properties of rare-earth metal oxyhydrides, explain the nature of the optical properties of these materials, understand their features driven by chemical and physical factors, suggest ways to improve their properties, and predict new promising compounds based on oxyhydrides.

2. STATE-OF THE ART OF STUDY ON MULTI-ANION MATERIALS

2.1. On systematics of multi-anion materials

A solid whose crystal lattice contains two or more anions belongs to the class of multi-anion systems. The most known families are: oxyhydroxides (or oxide-hydroxide) [13, 14, 15], oxyfluorides (oxide-fluoride) [19, 20, 21, 22] and oxynitrides (oxide-nitride) [16, 17, 18]. Condensed systems of the type $Re_xH_yO_z$, where Re is a trivalent rare-earth element, form a class of oxyhydrides (oxide-hydride) [23, 24]. Unlike binary compounds such as oxides, fluorides, nitrides, and hydrides, whose structures consist of simple building blocks, a multi-anion compound acquires new degrees of freedom due to differences in such characteristics as valence, ionic radius, and electronegativity. [11, 12]. Table 1 illustrates a comparison of the individual characteristics of several nonmetals. The utilization of these degrees of freedom through various chemical combinations opens up more possibilities to control and modify the structural and electronic properties of a material synthesized as a multicomponent compound according to the "cation + anion1 + anion2 + ..." scheme. As for the case of two anions, such a scheme is graphically illustrated in Figure 1 for the Y-H-O system. In the thesis, our primary interest is a detailed study of oxyhydride systems in which two anions, O^{2-} and H^-, together with a rare-earth metal cation share a common chemical space.

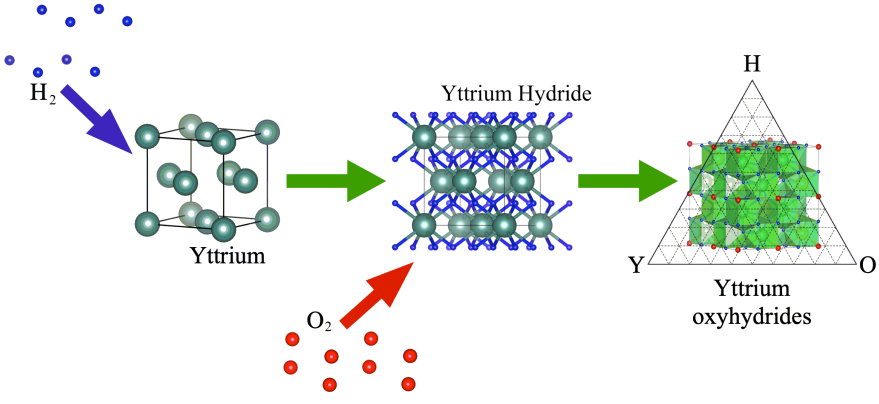

Figure 1. Schematic diagram illustrating the Y-H-O oxyhydride system [1].

2.2. Synthesis of metal oxyhydrides

It is known from the chemistry of metal hydrides that (i) their decomposition at high temperatures occurs with the release of molecular hydrogen H_2 [53, 54, 55], and (ii) the interaction of metal oxides with H_2 usually leads to the complete reduction of the oxide to the metallic state [56, 57]. The idea of using unsaturated versions

Table 1. Atomic characteristics shown in terms of the charge, atomic mass (in amu), electron affinity (in kJ mol^{-1}), ionic radius of anion (in pm) and Pauling electronegativity (all the data are taken from Ref. [47, 48, 49, 50, 51, 52].

Atom	Anion shell config.	Anion charge	Atomic mass (amu)	Electron affinity (kJ mol^{-1})	Ionic radius of anion (pm)	Pauling electro-negativity
H	$1s^1$	-1	1	72.8	134	2.20
F	$2s^2 2p^5$	-1	19	328.2	129	3.98
Cl	$3s^2 3p^5$	-1	35.5	348.6	167	3.16
O	$2s^2 2p^4$	-2	16	141.0	135	3.44

of a metal hydride as a starting compound to make its oxyhydride was proposed by Fokin et al [28, 29, 30]. The synthesis was realized by partial oxidation of MH_x (M = Ti, Zr, Sc, Y, V) metal hydrides with molecular oxygen. These compounds in the form of dihydrides were first obtained by hydrogenation of their iodides at 550 C and hydrogen pressure of 1 - 1.5 MPa, and then they were converted to monohydride phases by calcination at 600 C under a vacuum of 1 Pa. Next, oxidation with molecular oxygen at 1 MPa and heating to 330 C was performed. To find different stoichiometric configurations, the time of this operation varied from 5 minutes to 3 hours.

The experimental work of Kageyama's group [58, 59, 60] on the synthesis of several oxyhydride compounds crystallizing in spinel- and perovskite-like structures was based on the topochemical reduction of initial oxides followed by the removal of undesirable byproducts. The key feature of this method is that it does not require high temperatures and pressure. By means of topochemical reactions it also became possible to synthesize oxyhydride derivatives of titanates, (Ba, Sr, Ca, Eu)$TiO_{3-x}H_x$ [61, 62, 63], cobaltate $LaSrCoO_3H_{0.7}$ [64] and vanadate $SrVO_2H$ [65]. The opportunity to perform the high pressure direct synthesis from the initial mixture of hydride and oxide compounds was also utilized. The high-pressure effect, which prevented the release of gaseous hydrogen H_2, enabled this solid-phase synthesis of such metal oxyhydrides as $LaSrMnO_{3.3}H_{0.7}$ [66], Sr_2VO_3H [67] and $SrCrO_2H$ [68].

A research group led by S. Karazhanov developed and implemented another approach to the synthesis of stable yttrium oxyhydrides, which enabled to obtain thin oxyhydride films of different chemical compositions [25, 69, 70]. According to the reported method, the preparation of the two-anion oxyhydride system consists of two stages: deposition of yttrium hydride on a glass substrate in the unsaturated form YH_x in the first stage and subsequent oxidation by atmospheric oxygen in the second stage. The schematic flowchart of obtaining the material is illustrated in Figure 2. The deposition of YH_x thin films is provided at a low pressure of 10^{-1} Pa by magnetron sputtering of a pure metallic yttrium target in a flow of argon and hydrogen gases mixed in a ratio of about 8 : 1. In the second stage, the deposited YH_x is exposed to an air atmosphere to introduce oxygen into the film. The amount

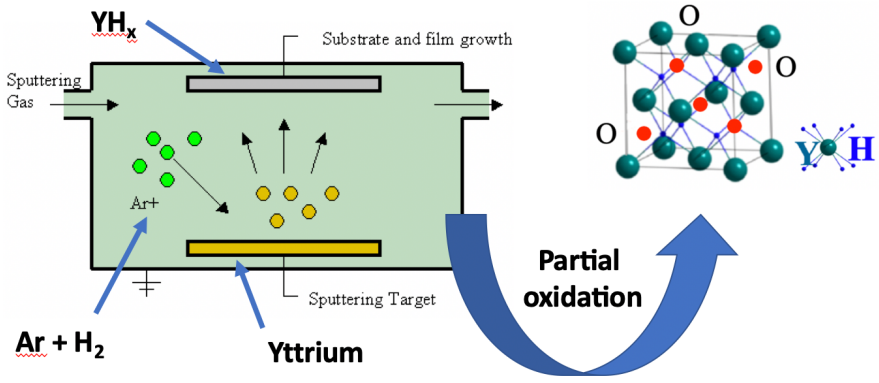

Figure 2. Schematic view of the synthesis mechanism of yttrium oxyhydride thin films, fabricated by partial oxidation of yttrium hydrides which were obtained by magnetron sputtering.

of oxygen absorbed depends on the exposure of the sample to air (up to several hours to obtain the maximum oxygen content). That is, the lighter the sample with respect to its light transparency, the more oxygen is chemically bound in the bulk structure. Moreover, to obtain a homogeneous yttrium oxyhydride composition throughout the sample, the substrate carrier functions in oscillation mode in front of the yttrium target [36].

2.3. Study of the properties of yttrium oxyhydhrides

The most attractive feature of a multi-anion compound is the possibility of flexible control of the structure-property relationships [12, 23, 24, 31]. The enlargement of the number of degrees of freedom due to the integration of additional oxygen anions into the yttrium hydride matrix adds more functionality to these materials. Moreover, a smooth adjustment of the synthesis conditions may make it possible to obtain multi-anion materials with controlled stoichiometry. Thus, an important task is to clarify how changing the oxygen concentration in yttrium hydride films can affect the structural, electronic, and optical properties of the oxyhydrides.

2.3.1. Chemical formula for yttrium oxyhydride

The chemical formula of the stable yttrium oxyhydride composition has been the subject of much debate for a long time. For the first time the chemical formula was suggested by Pishtshev and Karazhanov in Ref. [31]. In order to take into account the incorporation of oxygen via the H-O substitution, two hydrogen atoms occupied interstice positions of the original YH_3 fcc-lattice were replaced by one oxygen atom. Such theoretical model corresponded to a chemical composition of $YH_{3-2x}O_x$ with x=0.25, which is very close to an approximate composition of $YH_{2.4}O_{0.3}$ proposed in Ref. [42]. Next, screening of oxygen position preferences was carried out together with full geometrical optimization. It was found, that the

relaxed lattice parameter a=5.233 of the equilibrium structure $YH_{2.5}O_{0.25}$ agrees well with the experimental value of a = 5.24 [42]. Subsequently, this result was experimentally confirmed by Netherlands group [71, 72]. Later, the chemical formula $YH_{2-x}O_x$ was suggested as a result of a systematic composition analysis carried out in Ref. [38] using time-of-flight elastic recoil detection analysis (TOF-ERDA).

2.3.2. Correlation of oxygen content with stoichiometry and crystal structure

In work [37], the aim was to investigate the relationship between the chemical composition of Y-H-O thin films and their key properties. For this purpose, a sample of yttrium oxyhydride thin film was prepared with varying oxygen concentration along the length. The images given in Figure 3 show the optical behavior of the Y-H-O thin-film sample in which the color changes from black opaque when oxygen content is low to transparent when oxygen content is high. Two different states corresponding to the composite (two-phase) metal/insulator film were experimentally observed: the first picture in the upper panel was taken immediately after exposure to air (about 2 hours after deposition), and the second picture in the lower panel was taken after the sample was exposed to air 57 days after deposition. It can be seen that the edge of the black opaque part of the sample has shifted 10 mm to the left due to changes caused by further oxidation. Measurements of oxygen levels along the length of the sample showed a gradual increase in the average bulk ratio [O]/[Y] from 0.25 for the (left) black region to 0.65 for the transparent region. These data are also in good agreement with the results of the elastic energy recoil detection analysis and nuclear reaction analysis reported in the paper [41]. In addition, this sample of yttrium oxyhydride film was investigated by X-ray diffraction analysis. Measurements were done along the lateral direction of the film for a number of positions from 5 to 70 mm spaced in 5 mm intervals. The obtained GI-XRD diffraction patterns are shown in Figure 4a. Based on XRD experiments, the crystal structure of both the black (opaque) and yellow (transparent) regions of this yttrium oxyhydride sample was classified as matching cubic symmetry. This result confirmed the conclusions of the previous XRD analysis [25].

Thus, the dependence of the metal-dielectric transition on oxygen content becomes a dominant effect as more and more oxygen is chemically and structurally incorporated into the hydride lattice. The interesting fact is that the addition of oxygen causes an expansion of the host structure. Figure 4b shows an enlarging of the lattice parameter with the increase of oxygen content. It can be seen that as the color changes from opaque black to transparent yellow, the average lattice constant gradually rises from 5.27 to 5.34 Å. The compositional characteristics of yttrium oxyhydride films were investigated using the Time-of-Flight/Energy coincidence Elastic Recoil Detection Analysis (ToF-E ERDA) spectra [40]. The features of the

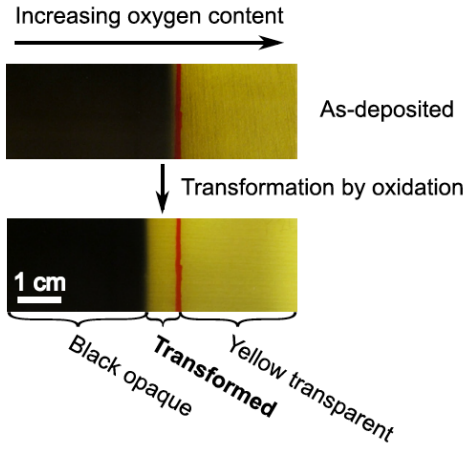

Figure 3. Optical behavior of Y-H-O metal/insulator composite film as a function of time. The upper image corresponds to the experiment completion time, the lower one – after 57 days. Reprinted from [37] with permission from Elsevier. License Number 5084811379232.

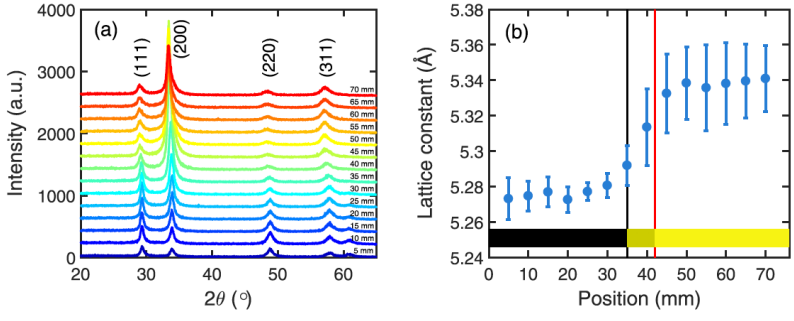

Figure 4. GI-XRD studies of Y-H-O metal/insulator composite film [37]. (a) GI-XRD patterns measured at different positions. The major diffraction peaks correspond to the (111), (200), (220) and (311) orientations. (b) Change of the lattice parameter versus oxygen content (as specified by the position on the sample). The colors are defined in the caption to Figure 3. Reprinted from [37] with permission from Elsevier. License Number 5084811379232.

spectral behavior for the individual components of the oxyhydride composition are demonstrated in Figure 5. The depth profiles of the atomic concentrations of yttrium, oxygen, and hydrogen were measured for both surface and bulk regions. A careful comparison of the obtained spectra allowed the authors of the paper [40] to conclude that the chemical transformation into an oxyhydride composition occurs according to the standard route of the oxidation process, when hydrogen is partially replaced with oxygen, and the balance of charges is ensured by the fact that the amount of Y remains at the same level. Besides, it was ascertained that light illumination has no effect at all on the atomic concentration of yttrium, oxygen and hydrogen in the Y−H−O system.

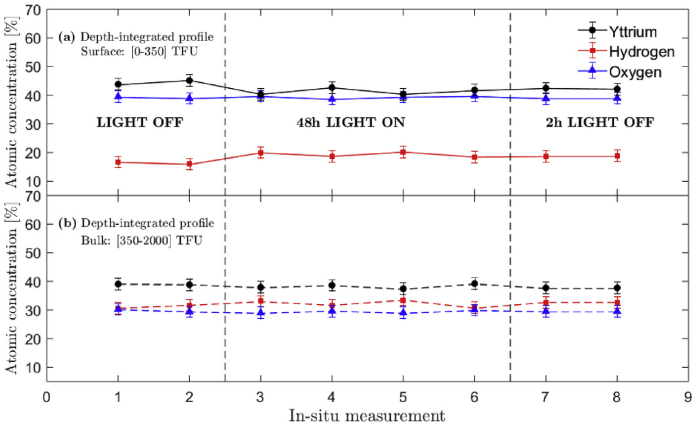

Figure 5. The results of ToF-E ERDA investigation for the yttium oxyhydride film [40]. Depth-integrated profiles associated with the Y, H and O atomic concentrations are given for three regimes of light illumination: before (light off), during 48 hours (light on) and 2 hours after (light off). (a) The surface region – [0–350]$\times 10^{15}$ at/cm^2; (b) the bulk region – [350–2000]$\times 10^{15}$ at/cm^2. Reprinted from [40] with permission from Elsevier. License Number 5084821024631.

The synthesis of an orthorhombic phase of bulk yttrium oxyhydride in the high-oxygen composition YHO was reported in 2019 [73]. The crystal structure of this material, corresponding to the anti-LiMgN structure type, possesses *Pnma* space symmetry, which has been confirmed by powder neutron and powder X-ray diffraction measurements.

2.3.3. Electrical properties

The photoinduced electrical resistance was measured for the black and transparent regions of the yttrium oxyhydride composite sample (which has already been mentioned above as well as in Figure 3) [37]. Figure 6a illustrates how the resistivity grows with increasing oxygen content in yttrium oxyhydride, showing a sharp drop in conductivity between the black opaque and transparent yellow regions, which relates to the metal-dielectric transition point controlled by oxygen. The lowest resistivity value $\rho = 10^{-2}$ Ωcm observed in the leftmost position of the figure panel corresponds to the region with the lowest oxygen content, which is characterized by a metallic ground state. Further reduction of the [O]/[Y] ratio allows synthesis of more electrically conductive yttrium oxyhydride films, which exhibit $\rho = 10^{-3}$ Ωcm [25, 36]. The metal-dielectric transition (i.e., the switch from a black opaque state to a yellow transparent state, as depicted in Figure 6a) is accompanied by a significant increase in resistivity of about four orders of magnitude; a feature which is also typical of other REM oxyhydrides, such as GdO_yH_x [35, 74]. The strong jump in resistivity is associated with the opening of the interband gap, which occurs in the electronic subsystem when the component ratio [O]/[Y] in the yttrium oxyhydride composition becomes greater

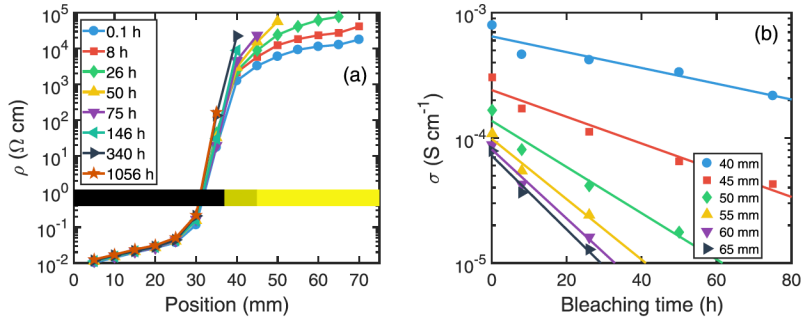

Figure 6. (a) Photoinduced electrical resistivity of yttrium oxyhydride sample measured for different bleaching times [37]. The colors are defined in the caption to Figure 3. (b) Photoconductivity as a function of brightening time, measured at different positions to reflect variations in oxygen content. The solid lines represent the best fit to the experimental data. Reprinted from [37] with permission from Elsevier. License Number 5084811379232.

than $\sim$0.2. As found in the experiment, the highest resistivity value, $1.8 * 10^6$ Ωcm, corresponds to the region with a high oxygen content, which represents the dielectric ground state, characterized by the yellow transparent region in Figure 6a. Figure 6b demonstrates changes in photoconductivity σ for different positions on the yttrium oxyhydride sample as a function of bleaching time. It can be seen that a variation of photoconductivity by at least one order of magnitude can also be achieved by adjusting the bleaching time.

2.3.4. Electronic states and optical properties

The valence states of yttrium oxyhydride were studied by X-ray photoelectron spectroscopy (XPS). Figure 7 shows the experimental XPS spectra both for black opaque and transparent yttrium oxyhydride samples, which are compared with the XPS spectra measured for yttrium hydrides, yttrium oxide, and metallic yttrium [27]. Comparison of the spectra revealed the presence of a stable (chemically bound) amount of oxygen in all yttrium oxyhydride samples. The band gap value estimated from the experimental valence band spectrum for the transparent sample was about 4 eV, which agrees well with the results of other measurements [43, 76].

Optical properties of the yttrium oxyhydride thin films are described in Figure 8 which demonstrates spectral properties of the refractive index (n) and extinction coefficient (k) in dependence on light wavelength λ in the interval between 300 and 1700 nm [45]. As one would expect, at longer wavelengths the optical behavior of the black opaque yttrium oxyhydride samples (designated $S1$ and $S2$ in Figure 8) is characterized by a nonzero extinction coefficient, which is caused by the Drude contribution to conductivity [78, 79, 80]. For the transparent samples ($S3$, $S4$, and $S5$ in Figure 8) in the wide spectral range above the fundamental absorption edge, the refractive index decreases smoothly with increasing wavelength. This behaviour is typical for semiconductor and dielectric materials [81, 82]. For example, the observed behavior of the refractive index in transparent yttrium oxyhydride is

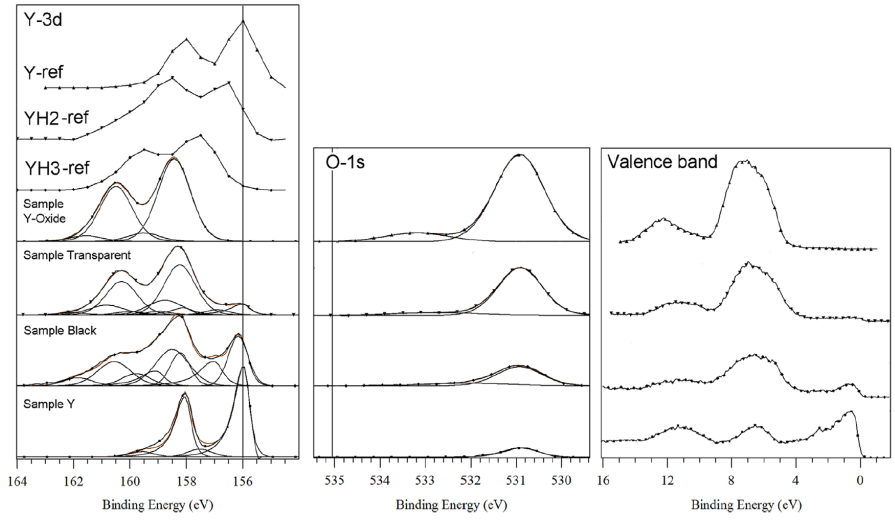

Figure 7. Comparison of the experimental XPS spectra measured for black opaque and transparent yttrium oxyhydride samples [27] with reference spectra of compounds Y, YH_2 and YH_3 [75]. The presence of oxygen in the oxyhydride samples is demonstrated in terms of the O-1s core levels. Reprinted from [27] with permission from Elsevier. License Number 5084830028304.

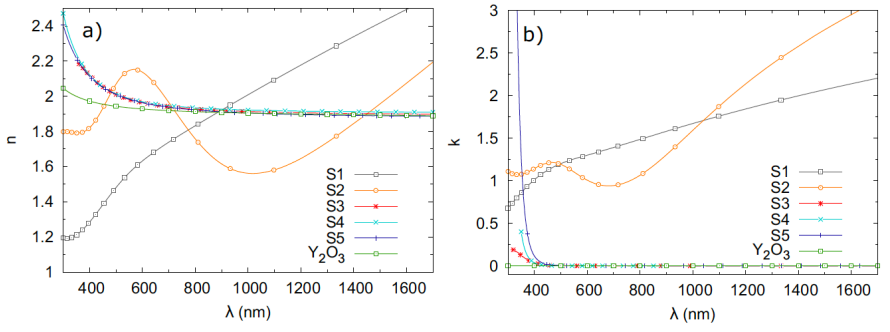

Figure 8. Refractive index n (left figure) and extinction coefficient k (right figure) determined for yttrium oxyhydride thin films of different thickness and different deposition conditions [45]. The measurements designated as $S1$ and $S2$ and the measurements designated as $S3$, $S4$ and $S5$ correspond to the experiments performed for black opaque and transparent samples, respectively. For comparison, the figure additionally illustrates the data for $n(\lambda)$ and $k(\lambda)$ obtained for pure Y_2O_3 oxide [77]. Reprinted from [45] with permission from John Wiley and Sons. License Number 5084830449345.

similar to that described for a wide band gap yttrium oxide [77].

The transmission (T) and absorption (A) spectra of transparent yttrium oxyhydride thin films deposited at different pressures in the magnetron sputtering chamber are shown in Figures 9a and 9b, respectively [43]. Figure 9a shows that the samples synthesized at a higher deposition pressure have better optical transmission. That is, increasing the deposition pressure leads to a shift of the

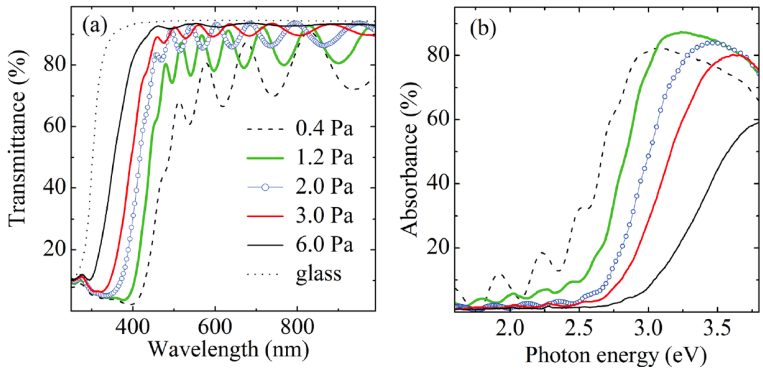

Figure 9. Optical properties of transparent yttrium oxyhydride thin films. Transmission (a) and absorption (b) spectra were measured for the samples deposited at various argon/hydrogen pressures ranging from 0.4 to 6.0 Pa [43]. Measurements of a glass substrate are also included as a reference. Reprinted from [43] with permission from AIP Publishing. License Number 5084831382961.

absorption band edge toward shorter wavelengths. The absorption spectra shown in Figure 9b demonstrate how the optical interband gap consistently increases with increasing deposition pressure. Analysis of the transmission and reflection spectra (R) of yttrium oxyhydride films showed that the optical band gap can be in a wide range of values 2.8 – 3.7 eV [25]. The widening of the optical band gap is directly related to the oxidation effect, when more oxygen added increases the ionic contribution in the chemical bonds [43]. As an illustration of the oxygen-induced modification, it is interesting to note that the aforementioned optical band gap values determined for yttrium oxyhydrides [25] are between the 2.6 eV value known for pure yttrium trihydride YH_3 [83] and the 5.5 eV value known for ionic Y_2O_3 [84]. From a practical point of view, this possibility to control flexibly the band gap width and optical properties by changing the oxygen content makes rare-earth oxyhydrides promising materials for further use in the development of optoelectronic applications.

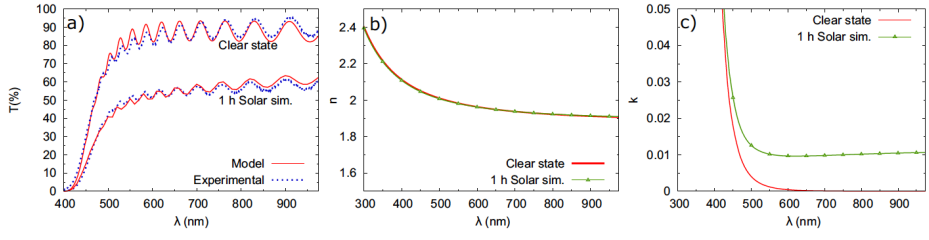

Figure 10. Illustration of the photochromic response in yttrium oxide film [45]. (a) Optical transmittance measured before and after 1 hour of illumination. (b) and (c) – Change in spectral behavior of refractive index and extinction coefficient, respectively, with illumination. Reprinted from [45] with permission from John Wiley and Sons. License Number 5084830449345.

One of the interesting optical effects demonstrated by transparent yttrium oxy-

hydride thin films is their ability to change transmittance when illuminated by light [27, 36, 43]. This specific feature of darkening of the material under the influence of light underlies the photochromic effect [85, 86, 87, 88]. A thorough study of the effect in oxyhydride systems was initiated in 2011 by two research groups – in Norway and in Netherlands [25, 26]. Although much attention has recently been paid to the study of the photochromic response in various oxyhydrides [37, 38, 42, 69, 72, 76], the physical mechanism of light-induced darkening is still a subject of considerable discussions. In this regard, it is interesting to mention the experimental work [45] in which the optical properties of transparent yttrium oxyhydrides were investigated both before and after 1 hour of illumination in a solar simulator calibrated to 1 of the Sun. The results shown schematically in Figure 10 allowed the authors [45] to present the genesis and evolution of the photochromic response in yttrium oxide film in terms of the optical behavior of a composite system – a macroscopic wide-gap matrix in which the creation and dynamics of metal domains are regulated by light.

3. THEORETICAL METHODS

3.1. Discrete symmetries of solids

The crystal structure of solid materials can be described as a combination of the basis, a set of atoms arranged in a certain way, and the lattice, which determines the repeating (periodic) configuration of the crystal (translational symmetry). A schematic representation of the crystal structure of a solid is shown in Figure 11 [89, 90]. The basis can also be defined as the set of points in a unit cell, the smallest repeating unit possessing an entire symmetry of the crystal structure. Geometrically, a unit cell can be described as a traditional parallelepiped represented by six variables – the lengths of the cell faces (a, b, c) and the angles between them (α, β, γ).

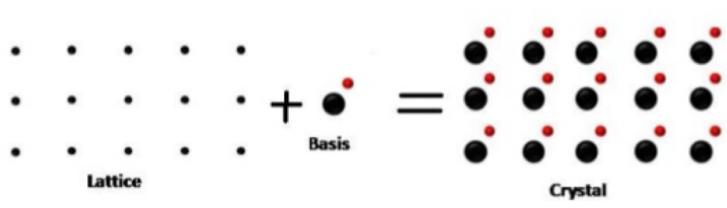

Figure 11. Schematic view of the crystal structure of a solid represented in terms of composition of a basis, a set of atoms arranged in a particular way, and a lattice [89, 90].

From a fundamental point of view, it is important that the ordered arrangement of atoms in a unit cell can be objectively characterized by discrete symmetry operations. A symmetry operation is defined as a formal action of a transformation that does not change the crystalline object after the action has been completed (i.e. its structure remains invariant under the given transformation) [91, 92, 93]. According to the particular configuration of atoms in a given discrete structure, only certain combinations of symmetry elements can be associated with a crystal lattice. As a result, it is possible to group atoms with the same symmetry elements and classify crystals according to their symmetry. A complete set of symmetry elements (such as translation, reflection, rotation and inversion) allows us to classify the ordering of atoms in a crystal body in terms of 7 crystal systems, 14 Bravais lattices, 32 point groups and 230 space groups [94, 95, 96, 97, 98, 99, 100, 101].

3.1.1. Characterizaton tools

The software tools [102, 103] hosted by the Bilbao Crystallography Server [104, 105, 106] present a set of various applications of group theory that can be successfully applied to describe symmetry in a crystal, analyze lattice structure, study the symmetry properties of electronic structure and classify vibrational modes, to understand possible structural transformations and phase transitions in crystals, *etc*. The Bilbao Crystallography Server is an open-access website that runs an online crystallographic database and software dedicated to the analysis, calculations, and

visualization of problems of structural and mathematical crystallography, solid state physics, and crystal chemistry (Figure 12).

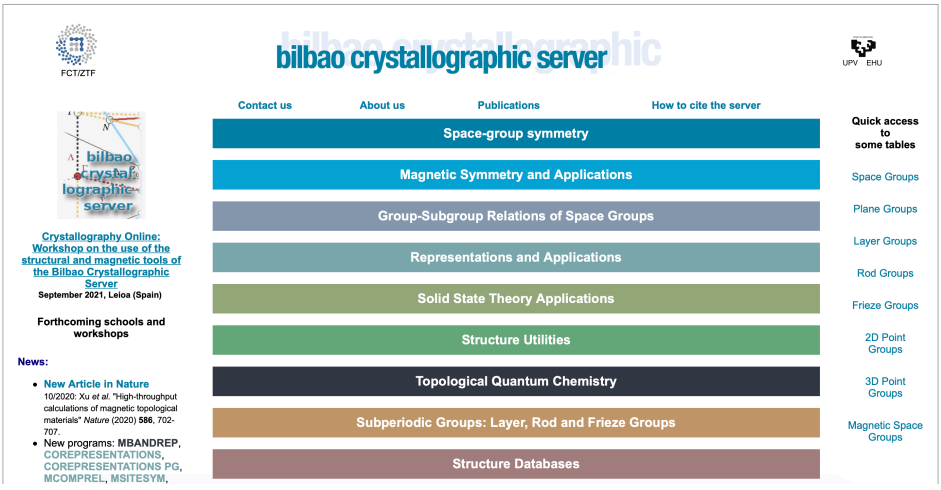

Figure 12. Screenshot of the main web-page of Bilbao Crystallographic Server [104, 105, 106].

VESTA software [107, 108, 109] has been used for three-dimensional visualization and exploration of various crystal structures as well as for simulation of volumetric (voxel) data such as X-ray diffraction patterns [110].

3.2. Vienna Ab initio Simulation Package (VASP)

The Vienna Ab initio Simulation Package (VASP) [111, 112, 113, 114, 115] is scientific software that has been developed to perform computer simulations of materials at the atomic level, including electronic structure and optical response calculations as well as quantum mechanical molecular dynamics. The modeling can be done either by using density functional theory (DFT), solving the Kohn-Sham equations, or by using the Hartree-Fock (HF) approach. VASP also involves calculations with hybrid DFT functionals [116, 117, 118] that account for a certain portion of the Fock exchange [119, 120, 121, 122], and also includes the use of the Green's function method, which is implemented at different levels of the GW approximation [123]. The GW approximation, which represents a first-principles implementation of the many-body approach, can be used to model excited states in solids in terms of quasiparticle excitations in order to describe the electronic band structure and the frequency-dependent dielectric function [124, 125]. In the calculations, the VASP code uses its own atomic pseudopotentials, enhanced by the projector augmented wave functions [126].

3.2.1. Stability analysis

The structural and dynamic stability of lattice configurations is determined with respect to the following criteria. First, it is necessary to calculate the squares of the zone-centered vibrational modes, since their positive values confirm the stability of the lattice with respect to the relative displacements of the crystal sublattices [127, 128] Second, the macroscopic stability of the crystal structure must be verified by an analysis of the total positivity of the elastic energy; such a confirmation is carried out through a study of the eigenvalues of the elasticity tensor (stiffness matrix) [129, 130]. The theoretical study of thermodynamic stability uses the results of accurate DFT calculations of the free energy, which allow us to estimate both the formation energies for a given structural composition and to verify the chemical stability with respect to the corresponding decomposition reactions.

3.2.2. Examination of elastic properties

The open-source online application ELATE [131] is a software tool with the functionality to calculate, analyze and visualize elastic properties for any periodic solid. As input data, ELATE takes a 6×6 symmetric matrix of second-order elastic constants, C_{ij} (written in the Voigt notation, and the units are GPa). In the representation of three averaging schemes (Voigt [132], Reuss [133] and Hill [134]), the program evaluates and displays such material properties as bulk modulus, Young's modulus, shear modulus and Poisson's ratio. The six eigenvalues of the elasticity tensor are also calculated. If at least one of them is negative, the elasticity tensor is not uniquely positive; this means that the system is structurally unstable [129, 135]. For structurally stable systems, the program also provides information on the spatial behavior of elastic moduli: Young's modulus (E), linear compressibility (β), shear modulus (G) and Poisson's ratio (ν). The results of extended tensor analysis can be very useful in the search for materials with desired or anomalous elastic properties, such as those with negative linear compressibility [136], negative Poisson's ratio (partial or total auxeticity) [137, 138], or highly-anisotropic elastic moduli [139].

4. RESULTS AND DISCUSSION

4.1. Materials modeling [Paper VI]

> "The fundamental laws necessary for the mathematical treatment of a large part of physics and the whole of chemistry are thus completely known, and the difficulty lies only in the fact that application of these laws leads to equations that are too complex to be solved."
>
> (Paul Dirac, 1929)

At present, a wide range of modern tools and methods, including evolutionary algorithms [140, 141, 142, 143], data mining [144, 145, 146], density functional theory [147, 148, 149, 150], molecular dynamics [151, 152, 153], *etc*, are used to predict crystal structures and investigate the main characteristics of materials. Many researchers systematically study various compounds in order to discover materials with unexpected properties or to develop new materials with desired properties. In the computational aspect, the capabilities of first-principle modeling have expanded significantly, allowing scientists to predict the structure and properties of advanced materials even before they will be synthesized. In general, the prediction of compounds with high accuracy must be combined with high-throughput screening methods, thus significantly advancing the search for new materials. There are, however, two marked disadvantages to such methods: the first is related to computational expenses, execution time and memory consumption, and the second is the fact that these methods cannot easily ensure that the results of crystal system simulations will meet the stability requirements.

In the present dissertation, we applied a method in which material modeling does not require any additional assumptions other than those that follow directly from symmetry considerations. Our strategy reflects the ideas of "local analysis" because the problem of modeling is transformed into a combination of associated subtasks satisfying the extensionality property – a one-way implication generates all possible inner configurations in accordance with the formal statement: model B is subset of model A. In the language of group theory, this means that model sequences are predicted by considering certain relationships between groups and subgroups and then evaluating the proper (most stable) configurations. For the given model structures, the calculations become mostly routine, and the matched configurations represented by the appropriate lattice geometries ensure good computational convergence. This provides significant economy of necessary computational resources and time. Besides, the formalization of material modeling gives a clear mathematical understanding of how the set of possible structural configurations can be considerably simplified, what, in turn, greatly simplifies the modeling itself.

4.1.1. Geometrization as realization of a fully geometric approach

The variety of natural and artificial crystals shows that the world of crystals is characterized by a wealth of different phases and forms. To describe such an

amazing richness of crystal architectures, we will be guided by the fundamental idea that the patterns of structure reflecting the ordering of constituent elements (atoms, ions, molecular units) are governed by the symmetries of space groups [154, 155, 156]. According to Felix Klein's Erlangen program (e.g., [157]), any geometry should be realized as a theory of geometric invariants. In the constructive sense, geometric representation means that an arbitrary crystal system can be given a theoretical interpretation in terms of geometric abstractions and mathematical objects, such as finite groups. In other words, the model of crystal structure is considered not in terms of interactions between the constituent elements, but in terms of a discrete set of points, i.e. as a certain geometric configuration embedded in the three-dimensional Euclidean space E_3, as illustrated in Figure 13a. This

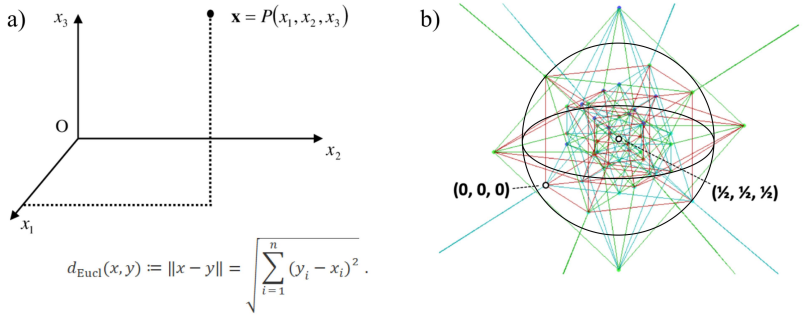

Figure 13. The geometric configuration illustrated in terms of (a) a metric space with distance function d, and (b) a set of operations of the octahedral group O_h .

figure schematically depicts a metric space with a distance function d given by the Euclidean norm, isometry, and geometric properties. A set of points can be mapped into this space by means of orthonormal Euclidean vectors generating primitive translations; the result of the mapping is a geometric configuration consisting of an abstract periodic lattice with a basis associated with crystallographic point groups. If G is a finite group from E_3, which we would like to engage within a discrete lattice model with on-site symmetry, we could consider arbitrary internal transformations based on the group of all rigid transformations T, passing to a factor group: $G/T \rightarrow SO(3)$. Here $SO(3)$ is a group of linear transformations represented as nontrivial rotations that preserve origin (when one point is chosen fixed), isometry, and orientation. Further, since the finite symmetry group does not assume elements such as translations or glides, the rotational group $SO(3)$ can be reduced to one of its finite subgroups to describe the symmetry properties of a given subset of discrete points that can be assigned to atom positions in a crystal unit cell. The focus of our interest will be the reconstruction of the crystal lattice as a highly symmetric geometric object whose symmetry is characterized by the full octahedral symmetry group O_h (Figure 13b). The motivation for choosing octahedral symmetry can be explained by the important fact that only two of the five fully space-filling convex polyhedra [158], the cube and the truncated

octahedron, have the highest symmetry; this particular symmetry belongs to the O_h group. Hence, to obtain periodic coverage of the entire three-dimensional space it is sufficient to fill it with copies of a single unit cell with octahedral symmetry. Another interesting fact is that in this case the resulting lattice packing has a density that is very close to the most optimal [159]. If a finite subset of discrete points from E_3 is a Delone set [160], then these points correspond to orbits under a proper crystallographic group. Thus, our goal is to consider the global symmetry properties of the lattice space (E_3, O_h), which we denote below as the configuration space of the geometrically projected three-dimensional discrete lattice. Given that the cube is dual to the octahedron, the cubic space group Fm-3m (no 225) will be taken to serve as the crystallographic group for all possible operations of the non-Abelian finite group O_h in this configuration space.

4.1.2. Lattice transformations

When we want to characterize a crystal as a real object whose chemical composition we know, we first of all describe its shape and structure. In our case, we will not focus on the typical lattice stability problem, where the structural configuration is governed by the delicate balance between the long- and short-range forces in the crystal lattice. We are going to consider structural/phase transformations from a geometric point of view, without regard to the microscopic mechanism of the transformation process, for example, in terms of the interaction of patterns (considered abstractly as geometric objects) and their discrete symmetries [156, 161]. Our geometric formalism concentrates on the characterization and classification of lattice configurations, their transformations, and orderings in terms of the evolution of discrete geometric objects. Our research work is based on the combined use of tools from discrete geometry and group theory to create and manipulate geometric models, as well as computational DFT tools to simulate these models in terms of structural variables, and to calculate material properties. Evolution is that the final choice of the most suitable substructures occurring in the hierarchy of structural configurations and generated by a given parent superstructure is made by comparing the efficiency/competitiveness of various pathways in the context of energy and stability conditions, which, in turn, are determined within the framework of accurate DFT-calculations. This approach keeps us from obtaining incorrect results, since it is quite safe to work with local transformation schemes, within which there is the possibility to freely move between model geometries and energy calculations at any time as needed. Figure 14A and Figure 14B [Figures 2A and 2B of Paper VI, respectively] provide a visual geometric insight into the variety of lattice configurations that a multi-anion chemical system can acquire as a result of molecular ensemble condensation. Constructive modeling of the results of this condensation by means of geometrical interpretation of possible structural phases relies on the classification of invariant chains of group-subgroup relations [162, 163]. Figure 14A illustrates a model of the initial distribution of ions over crystal-

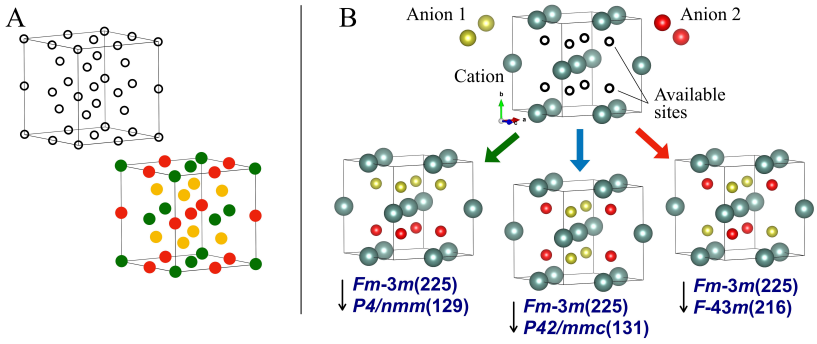

Figure 14. Crystallization of a two-chanion chemical composition, schematized by visualizing possible lattice configurations. The colored balls represent atoms occupying highly symmetric positions of the parent structure, the black circles correspond to empty areas that can be filled later. The colored arrows indicate three different transformations. (This figure corresponds to Figure 2 of Paper VI).

lographic sites. The model uses a rich set of discrete points (voids) available in the configuration space with high cubic symmetry O_h; not only can these voids be filled with atoms to form different cation-anion compositions balanced according to given crystallographic distributions, but their positions themselves can also be displaced under structural transformations. Figure 14B shows three possible directions in terms of group-subgroup relations, which determine the optimization of the parent cubic superstructure characterized by the space group Fm-3m (225).

4.2. Compositional and structural design

4.2.1. Y–H–O ternary phase diagram [Paper I]

The discovery of stable yttrium oxyhydrides initiated the study of various properties of these materials. In order to understand the synthesis methods and routes of formation of stable compositions upon condensation of the Y−H−O system, the relationship between the chemical composition and the crystal structure was theoretically modeled. The host metal hydride was chosen as the starting point in the simulation of the oxidation process; this allowed us to describe the appropriate structural transformations resulting in the formation of different structural phases. We have proposed an approach that can thoroughly model the results of oxidation of hydrides by oxygen incorporation and explain how the host lattice of a hydride compound can attach oxygen and increase its content in the unit cell up to the complete loss of structural stability. As a result, we predicted a number of condensed phases of several series of yttrium oxyhydride compositions, which are summarized in Figure 15 (Figure 1 of Paper I) and in Figure 16 (Figure 4 of Paper I). Modeling the properties of a multi-anion material showed that the functionality of a metal hydride can be regulated through a combination of different types of anions arranged in a common chemical space. This allowed us to understand the

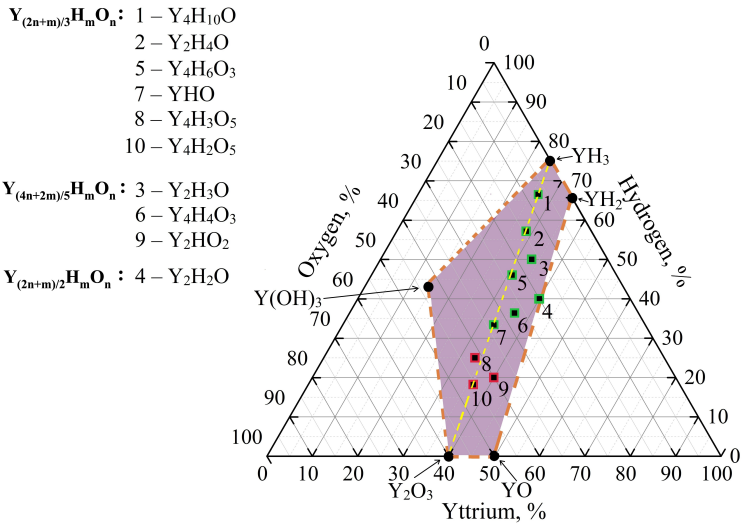

Figure 15. Phase diagram predicted for the ternary composition: the Y-H-O compositional triangle is outlined in terms of the variables Y, H, and O. Covered compositions are marked with black squares and numbered 1 to 10. The orange dashed lines connect end members Y_2O_3, YO, YH_2, YH_3, $Y(OH)_3$, and YO(OH). The union of intersections, shown as a solid pentagon, is an area of potential stability. The yellow dashed line connecting Y_2O_3 and YH_3 corresponds to a homologous series $Y_{(2n+m)/3}H_mO_n$ (Figure 1 of Paper I).

role of the combination of oxygen and hydrogen in yttrium oxyhydrides, which in fact turned out to be the main factor responsible for the formation and stabilization of the anion framework in the ternary lattice system.

4.2.2. Structural chemistry of REM oxyhydrides [Paper II]

An attractive feature of REM oxyhydrides is the possibility to change the structure-property relationships by affecting the hydrogen-oxygen ratio in the chemical composition. In this context, there is a perspective to trigger corresponding off-center displacements of cations and anions, which, by inducing a total asymmetry in the charge density distribution, can lead to the breaking of the inversion symmetry of the crystal structure. This opens the way to several polar systems in the homologous series $Ln_{2n+m}H_mO_n$ (Ln=Y,La), which can possess piezo- and ferroelectric properties. In Paper II we showed that the lower member of this series, the ternary system Ln_2H_4O, can crystallize in three noncentrosymmetric phases with monoclinic, orthorhombic, and trigonal structures. A schematic characterization of the layered topology of the polar Ln_2H_4O oxyhydride system is shown in Figure 17 (Figure 2 of Paper II). As it was revealed from our analysis, oxyhydrides of the given composition exhibit attractive electromechanical properties that can be used for the design and development of promising lead-free ferro- and piezoelectric systems.

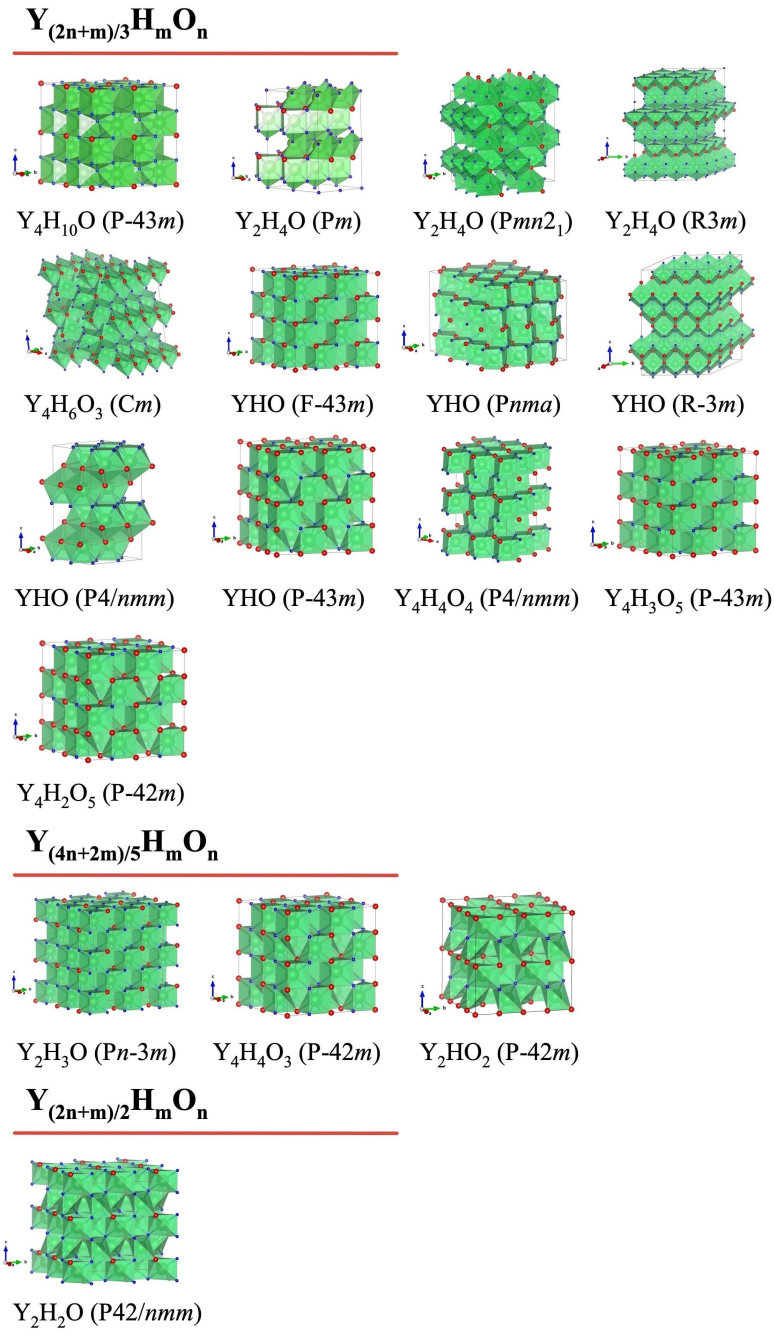

Figure 16. A variety of condensed phases of yttrium oxyhydrides. Here, yttrium, oxygen and hydrogen atoms are indicated as green, blue and red balls, respectively. The three-dimensional framework is rendered in terms of face-, edge-, and corner-sharing linkages of Y-H-O polydedra. All layers are stacked along the *c* axis [Figure 4 of Paper I].

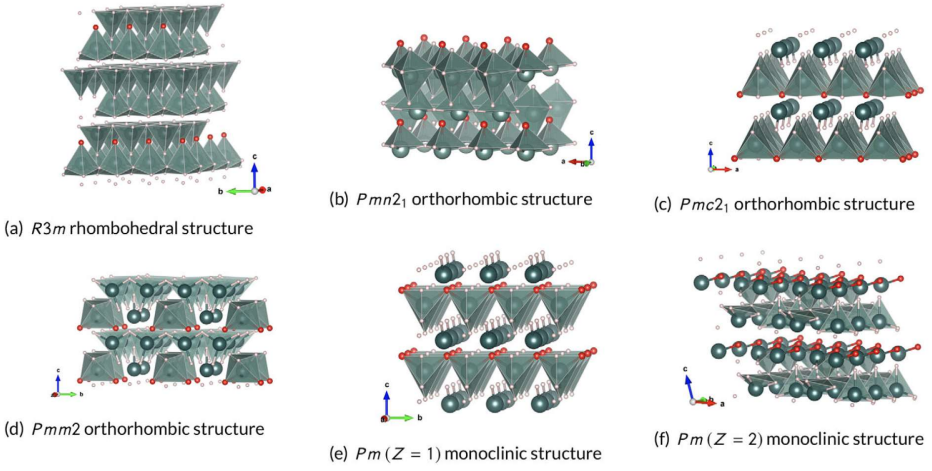

Figure 17. Layered topology of ternary Ln_2H_4O (Ln = Y, La) oxyhydride systems presented as polyhedral representations. Ln, O, and H atoms are drawn in dark green, red, and pink, respectively. (Figure 2 of Paper II).

4.2.3. Prediction of a new chiral material [Paper III]

Further search for possible ways of admixing oxygen atoms into the oxyhydride system led us to the prediction of a new class of inorganic crystalline materials - metal hydroxyhydrides, whose chemical composition $M_2H_3O(OH)$ (M = Y, Sc, La, and Gd) allows three different types of anions (H^-, O^2 and OH^-) to coexist in a common space. The symmetry of the material corresponds to the chiral space group $P4_1$. A schematic illustration of the predicted crystal structure of $M_2H_3O(OH)$ is shown in Figure 18 [Figure 1 of Paper III]; characteristic patterns of polyhedral chains are reproduced in Figure 19 [Figure 2b of Paper III]. The oxygen-induced proton displacements were found to be the result of oxygen-induced specific modifications in the crystal structure of $M_2H_3O(OH)$, which caused the charge state of some hydrogen anions to change from negative H^- to positive H^+, resulting in the formation of protonic centers in the hydroxyl groups. Due to the chiral structural organization of metal cations and anions forming helical curves in the tetragonal structure, the material exhibits a synergy of such effects as: extra-high localization of the valence charge density, dihydrogen bonding and stability of the coexistence of hydride and proton hydrogens in a common anionic framework. It is interesting to note that the dihydrogen linkage is caused by the twisting between negatively H^- and positively H^+ charged hydrogens, which are included in opposite chiral chains. The material properties of $Y_2H_3O(OH)$ were evaluated. Due to the "built-in" chirality, this material exhibits attractive optical characteristics: anomalous refractive index dispersion (Δn), as well as high absolute values of the second-order susceptibility tensor component $\chi_{zzz}(2\omega, \omega, \omega)$.

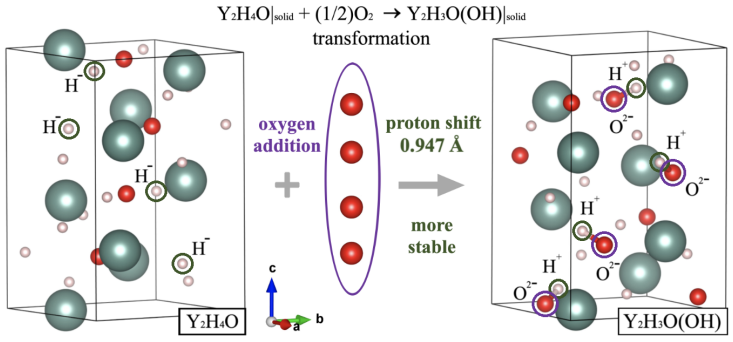

the reactant state

Atom	Wyckoff position	x	y	z
Y (1)	4a	0.31358	0.21131	0.42241
Y (2)	4a	0.29302	0.21792	0.00000
O (1)	4a	0.42484	0.36390	0.20738
H (1)	4a	0.01901	0.40569	0.08877
H (2)	4a	0.06431	0.47258	0.34710
H (3)	4a	0.11109	0.05559	0.21930
H (4)	**4a**	**0.17903**	**0.31074**	**0.68875**

Y – H(1)	Y – H(2)	Y – H(3)	Y – H(4)
2.138	2.179	2.322	**2.440**

the product state

Atom	Wyckoff position	x	y	z
Y (1)	4a	0.31438	0.20390	0.40665
Y (2)	4a	0.30949	0.21333	0.00000
O (1)	4a	0.42729	0.35803	0.20001
O (2)	**4a**	**0.18900**	**0.31295**	**0.65412**
H (1)	4a	0.01280	0.37473	0.06727
H (2)	4a	0.07726	0.46489	0.33691
H (3)	4a	0.10538	0.06210	0.19862
H (4)	**4a**	**0.26795**	**0.18978**	**0.70143**

Figure 18. Illustration of the rearrangement effect caused by the addition of oxygen: the visualization is presented as a comparison of elementary cells belonging to less stable and more stable compositions. The color codes of the atoms are: green – Y, pink – H, and red – O. Crystal packing models are shown in terms of positional characteristics. The H(4) and O(2) orbits which are active in the hydrogen migration are highlighted in green and in purple, respectively. The "lost" hydride hydrogen orbitals H(4) (left section) converted to protons (right section) are highlighted in green, and the newly added oxygen composing the O(2) orbital is highlighted in purple. The combination of orbits O(2) and H(4) generates four hydroxyl groups in the unit cell of $Y_2H_3O(OH)$ (Figure 1 of Paper III).

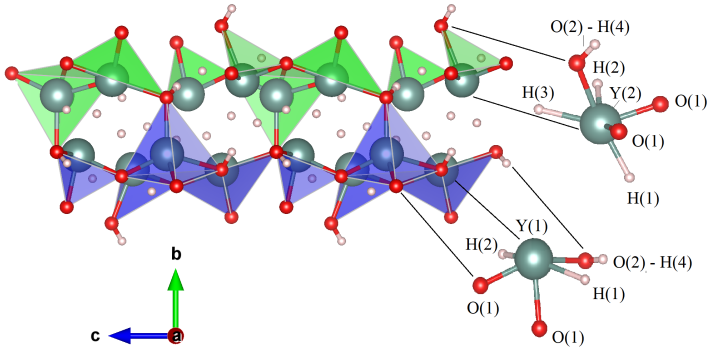

Figure 19. Part of the predicted crystal structure of $Y_2H_3O(OH)$: characteristic patterns of polyhedral chains displayed along the *a* axis. (Figure 2b of Paper II).

4.2.4. Electronic structure and optical properties [Papers IV & VII]

To understand how the electronic properties of the yttrium oxyhydride system can be associated with its chemical composition and structural properties, we compared the electronic band structure and density of states (DOS) calculated for the *P*-43*m* phase $Y_4H_{10}O$ and three different YHO phases described by the *F*-43*m*, *Pnma* and *P*-43*m* space groups, respectively. The results of calculations are presented in Figure 20. The low-oxidized version of the oxyhydride, $Y_4H_{10}O$, has a direct band

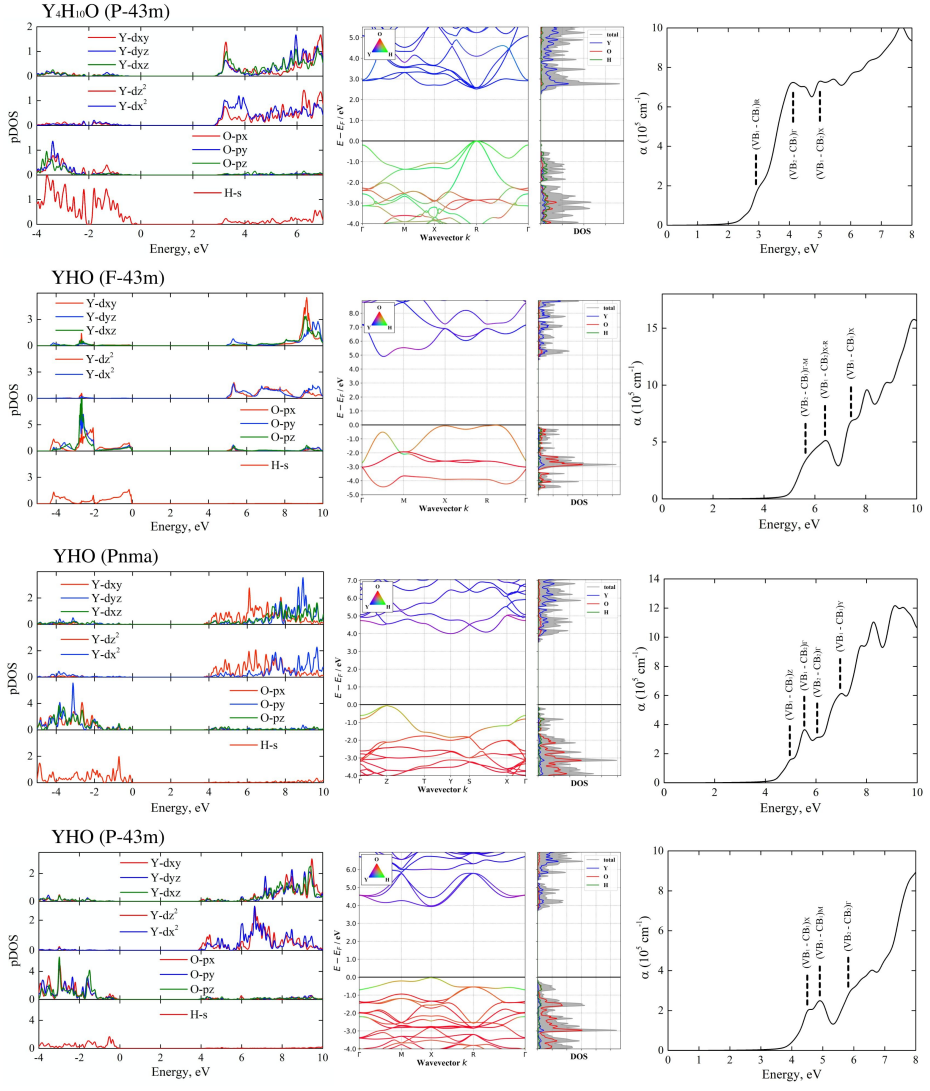

Figure 20. Site-projected density of states, electronic band structure along the high-symmetry directions of the irreducible Brillouin zone (BZ) and absorption spectra presented for $Y_4H_{10}O$ and YHO. The calculations were performed within the HSE06 hybrid functional. The Fermi level is set to the zero of energy.

gap with a valence band (VB) maximum and conduction band (CB) minimum located at the highly symmetric R of BZ. The top part of the valence band consists mainly of the hydrogen s-orbitals, which are separated from the lowest empty states belonging to the yttrium $4d$-orbitals, thus forming a fundamental band gap of 2.6 eV. The $2p$ states of oxygen hybridized with s electrons of H lie in the valence band with a shift to lower energies from the band edge by 1 and 3 eV, respectively. The calculated DOS picture is in good agreement with the spectral behavior of the absorption coefficient α presented in the right part of Figure 20. $Y_4H_{10}O$ exhibits almost zero absorption for photon energies below 2.2 eV. This value can be seen as an estimate of the optical band gap. Note that electronic transitions from the VB region with energies from -1 to 0 eV contribute little to the absorption spectra because these states are occupied by s-electrons of H, for which direct dipole transitions to yttrium $4d$ electronic states of CB are forbidden. The increase in absorption occurs at photon energies of 3 eV or higher, when the $2p$ oxygen states begin to contribute to the allowed $2p$-$4d$ interband transitions.

The calculations for strongly oxidized YHO, presented in Figure 20, describe the electronic band structures of three different phases. The F-43m cubic phase is characterized by an indirect wide band gap of 4.9 eV, which separates the VB maximum near the R point and the CB minimum located between the Γ and M points of BZ. This point of low symmetry also defines the smallest direct band gap of 5.5 eV. The uppermost part of the VB is formed by sp-hybridization of the electronic states of hydrogen and oxygen; the lowest part of the VB is completely filled with empty $4d$ states of yttrium with a small fraction of oxygen $3p$ states. The calculated absorption spectra ($\alpha(E)$ in the Figure 20) revealed almost zero absorption for photon energies below 5.0 eV. This value provides an estimate of the optical band gap for the F-43m phase of YHO. The electronic band structure of the *Pnma* orthorhombic phase of YHO has an indirect band gap of 3.9 eV separating VB and CB along the high symmetry points of BZ, Z and Y, respectively. The smallest direct band gap is 4.5 eV and belongs to the Z point of BZ. The uppermost part of BZ consists of hybridized s states of hydrogen and $2p$ oxygen, while the lowest empty $4d$ states of yttrium form the bottom of BZ. As can be observed in Figure 20, the optical band gap for the orthorhombic phase is $\sim$4.3 eV. The electronic band structure of P-43m cubic phase of YHO has a direct band gap of 4.0 eV, which separates the maximum VB and minimum CB at the high symmetry point X of BZ. The upper part of the VB consists mainly of oxygen $2p$ states hybridized with hydrogen $1s$ states, while the lowest CB states belong to the empty $4d$ electronic states of yttrium. For the given cubic phase, as can be seen from Figure 20, the magnitude of the optical gap, 4.0 eV, is identical to the fundamental gap. Note also that for all the three phase of YHO the significant growth of absorption spectra is associated with $2p$–$4d$ direct electron transitions between electronic shells of oxygen and yttrium, respectively. Note also that for all three phases of YHO a significant increase in the absorption spectra is associated with the activation of $2p$–$4d$ direct electron transitions between the electron shells of

oxygen and yttrium, respectively. Figure 21 [Figure 3 of Paper IV] compares

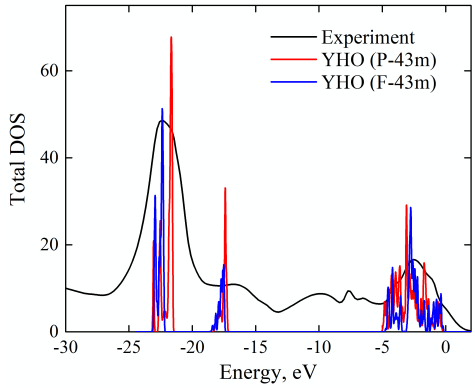

Figure 21. Comparison between the total DOS calculated for two cubic phases of YHO (*P*-43*m* and *F*-43*m*) and the experimental results of XPS measurements for thin film yttrium oxyhydride samples (Figure 3 of Paper IV).

the careful DFT calculations of the DOS with the experimentally measured X-ray photoelectron spectra. The total DOS picture was previously theoretically evaluated for both cubic phases YHO. As can be seen from Figure 21, the correspondence of the results allows us to suggest which structure the experimental sample has.

Figure 22 [Figure 1 of Paper VII] shows the optical properties of yttrium oxyhydrides, $Y_4H_{10}O$ and YHO, modeled based on the frequency-dependent real and imaginary components of the dielectric function, ε_{real} and ε_{img} respectively. Both of these components of the dielectric function were evaluated by DFT calculations using the hybrid HSE06 functional. The spectral behavior is presented for such optical characteristics as refractive index n, reflectance R and transmittance T. It is interesting to mention that $Y_4H_{10}O$ has a relatively high refractive index of 2.62 at 2 eV compared to ion-covalent materials with similar gap values. For example, the wide-gap semiconductor GaN ($E_g = 3.3$ eV) [164] exhibits a lower refractive index of 2.39 at the same incident light energy. For comparison, we note that strongly oxidized YHO has an even lower refractive index of 1.9 – 2.2 for incident light in the visible part of the optical spectrum. These low values are similar to those for wide-gap ion-covalent materials such as Y_2O_3 [165] ($E_g = 5.6$ eV, $n = 1.93$) and HfO_2 [166] ($E_g = 5.9$ eV, $n = 2.11$) metal oxides.

4.2.5. Ferro- and piezoelectricity [Papers II & V]

As we showed in Paper II, the reaching of structural stability through charge ordering in polar Ln_2H_4O oxyhydrides (Ln=Y,La) is provided by the strong interaction between different anion sublattices integrated into a rigid three-dimensional cationic framework. A study of the structure-property relationships for these systems revealed the unexplored potential of polar oxyhydride phases as promising lead-free piezoelectric materials. Using appropriate DFT calculations, we modeled such ferroelectric and piezoelectric characteristics of the Ln_2H_4O system as dielec-

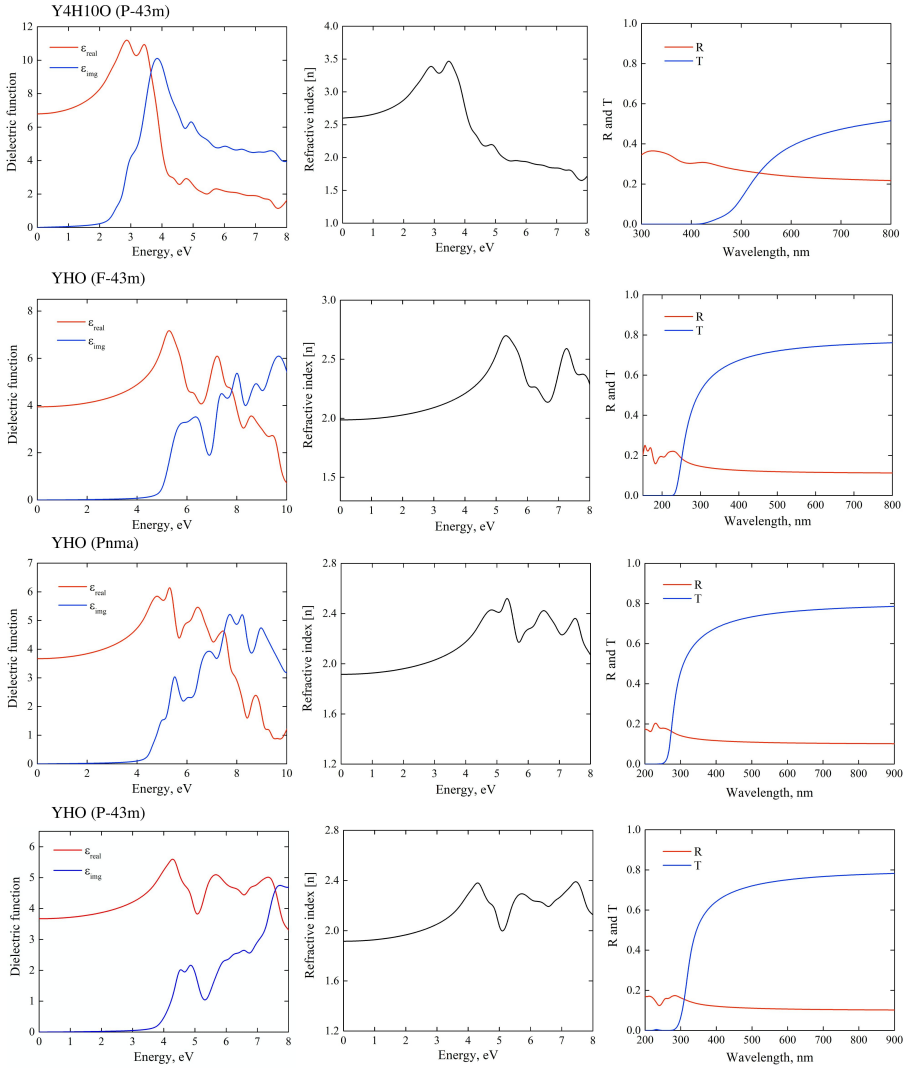

Figure 22. Optical characteristics of yttrium oxyhydrides $Y_4H_{10}O$ and YHO given in terms of frequency dependent dielectric function ε, refractive index n, reflectance R and transmittance T spectra (Figure 1 of Paper VII).

tric and piezoelectric tensors, macroscopic electric polarization, and also estimated several electromechanical characteristics; all are presented in Tables 4 – 6 of Paper II. Our predictions showed that the monoclinic and orthorhombic polar phases of Ln_2H_4O exhibit an outstanding piezoelectric response and can also provide energy harvesting capability. These characteristics are similar to those exhibited by known ferroelectric materials. Thus, Ln_2H_4O oxyhydrides may be of great interest as a starting point for the technological development of modern high-performance lead-free piezoelectric devices.

The study of substitution effects in polar REM oxyhydrides allowed us to

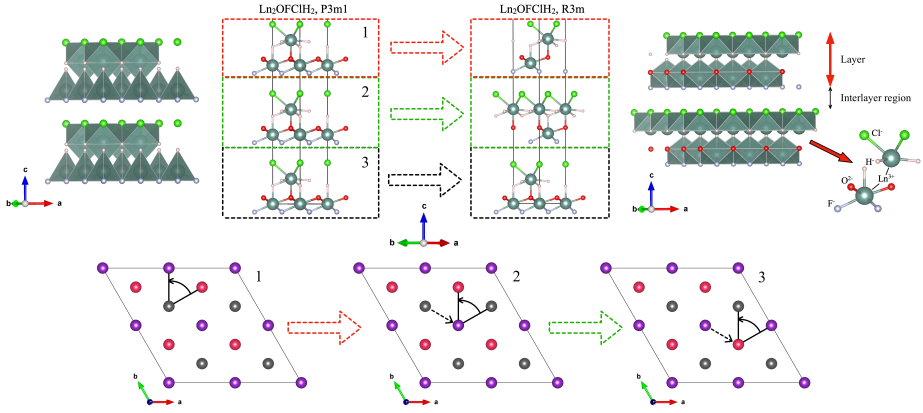

Figure 23. Illustrative 3*D* model of *P*3*m*1 and *R*3*m* phases of Ln_2OFClH_2. The model shows the profiles of the charged heteroatomic layers $LnHCl^{+1}$ and $LnOF^{-1}$ stacked on top of each other. Yttrium, oxygen, hydrogen, chlorine and fluorine atoms are indicated by dark green, red, pink, green and pearl balls, respectively. The polymorphic rearrangement between phases is represented schematically in terms of shear and rotation of atomic layers in the $[1\bar{1}0]$ crystallographic direction. (Figure 1 of Paper V).

predict a new family of multi-anion materials with the following composition: $Ln_2OF_{2-x}Cl_xH_2$ (Ln = Y,La,Gd). As illustrated in Figure 23 [Figure 1 of Paper V], this system $Ln_2OF_{2-x}Cl_xH_2$ crystallizes in the layered structures with the *P*3*m*1 or *R*3*m* trigonal symmetries. Two regularly stacked layers, LnO(FCl)H and Ln(FCl)FH, are arranged in alternating order along the polar axis *c*. The partial replacement of hydrogen anions by halogen anions caused a favorable anisotropic softening of the crystal lattice, which, by modifying the elastic characteristics, led to unique electromechanical characteristics. The bilayer configuration of different types of anions in the noncentrosymmetric trigonal structure generated a strong asymmetry of the valence charge density, which led to high electrical and mechanical responses to external loading. The unique combination of high piezoelectric response with enhanced elastic sensitivity may reveal the perspectives for the technological use of these $Ln_2OF_{2-x}Cl_xH_2$ based materials as low pressure sensors and powerful mechanical energy harvesters. In particular, their high electromechanical characteristics suggest that they may become direct competitors to piezopolymers such as PVDF.

4.3. Modeling of prospective devices [Papers II, III, V, VII]

The distinctive characteristics of rare-earth metal oxyhydrides have inspired the search for applications of these multi-anion materials. For example, the prediction of new inorganic materials with unique structural architecture, such as chiral metal hydroxyhydrides $M_2H_3O(OH)$, is of great interest for the development of novel optoelectronic and nonlinear optics (NLO) devices. Generally speaking, the

development of new inorganic materials with high NLO characteristics is one of the important challenges. Organic NLO materials generally do not exhibit good stability for hard conditions such as high electromagnetic fields, etc. Thus, the development of new chiral metal hydroxyhydrides $M_2H_3O(OH)$ with decent NLO properties may have great potential to overcome a number of existing problems and limitations and create a competitive material for high-power laser and photonics applications.

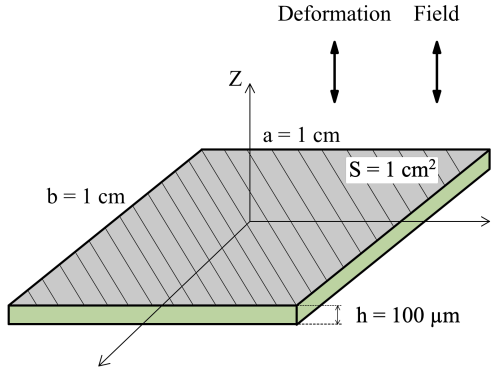

Figure 24. Illustrative view of the piezoelectric model of harvester which operates in the longitudinal mode (Figure 4 of Paper V).

The next idea in the context of a possible application was the flexible addition of different anions in order to create an internal channel of macroscopic charge asymmetry. The main focus in this direction was the specific configuration of partial substitutions, which led us to the heteroatomic anion $[OF_{2-x}Cl_xH_2]_6$. As a result, we proposed a polar material model Ln_2OFClH_2 (Ln = Y, La, Gd) that exhibits a unique combination of elastic and electromechanical characteristics. This model allowed us to develop the concept of an energy harvesting device that can combine the high piezoelectric power and softness typical of PVDF-type piezopolymers, on the one hand, and the high thermal and structural stability typical of solid piezoelectric ceramics, on the other. For example, our estimates of energy harvesting efficiency showed that the power output of a piezoelectric energy harvesting device produced by a system based on Ln_2OClFH_2 could be about 5-10 times greater than that of commercially available PZT-5H ceramic, and about 3-4 times greater than that of commercially available piezoelectric polymers. Illustrative view on piezoelectric harvester operating in the longitudinal mode is presented in Figure 24 [Figure 4 of Paper V]. Note also that the predicted material may be of particular interest for the development of the following electromechanical devices: (i) transverse stress sensing elements for monitoring applied mechanical loads, (ii) sensitive tactile sensors operating over a wide range of external forces from 0.01 to 1000 N, and (iii) a sensitive component of artificial skin models.

Also of interest from a practical point of view is the difference in the spectral behavior exhibited by different phases and compositions of yttrium oxyhydride in

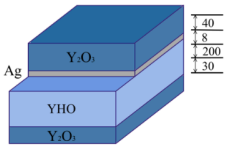

(a) Schematic view of the proposed model in a cross-section of layers. Layer thicknesses are given in nanometers.

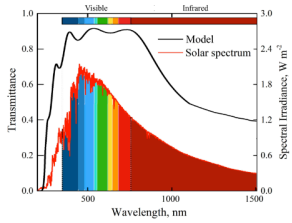

(b) Predicted transmittance spectrum *vs* available solar radiation. The solar spectrum was drawn on the base of solar irradiance data of Ref. [42].

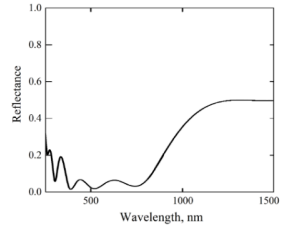

(c) Predicted reflectance spectrum.

Figure 25. Model of a low-emissivity coating. (Figure 3 of Paper VII).

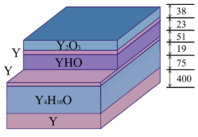

(a) Schematic view of the proposed model in a cross-section of layers. Layer thicknesses are given in nanometers.

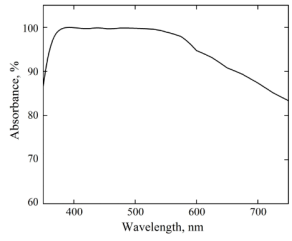

(b) Predicted absorbance spectrum.

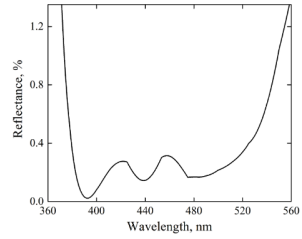

(c) Predicted reflectance spectrum.

Figure 26. Model of a light-absorbing non-reflective coating. (Figure 4 of Paper VII).

the optical range. Based on the obtained knowledge of the frequency-dependent complex dielectric function, reflection (R) and transmittance (T) spectra, a simulation of prototype composite optical systems designed on multilayer oxyhydride configurations was performed. By simulating the effects of refraction, transmittance, and reflection together with the effects of internal interference of light waves, we proposed two different prototype optical coatings in which yttrium oxyhydride thin films play a key role.

(i) *Model of a low-emissivity coating.* The idea is to propose a model that would block the ultraviolet (UV) radiation and, to some extent, the heating caused by the infrared (IR) component of solar radiation; the effectiveness of the model is determined by the fact that visible light can propagate with high transmittance (above 90%) and low reflectance (below 10%). The key details of the model are described in Figure 25a. The model reduces both UV and IR light radiation through a configuration that provides a "low-high-low" light transmission scheme (Figures 25b and 25c).

(ii) *Model of a light-absorbing non-reflective coating.* The idea is to propose a model that would exhibit high light absorption and low light reflection. The key details of the model are described in Figure 26. The main component of the model configuration is a metal-dielectric interface formed by a combination of yttrium and yttrium oxyhydride thin films; its target function is to significantly improve the

light-absorbing properties [167]. Another feature of this model is that its composite nature provides finding the proper combination of layer thicknesses to generate a composition for a broadband absorption coating with "ideal" absorption levels. In particular, in the case of normal incidence, simulation results showed that in the broader wavelength range of 375–550 nm, the system absorbs on average 99.7% of incoming light radiation; the highest absorption level, 99.98%, is reached at 395 nm. Worsening of the near-perfect absorptive property occurs at longer wavelengths of visible light, when the absorptivity gradually drops to 90%.

5. SUMMARY

The main purpose of the present PhD thesis was to study the oxyhydrides of the rare earth metals Y−H−O, La−H−O, Gd−H−O using a combination of theoretical and computational methods.

Using a combination of group theory methods, multi-anion chemistry reasoning, and density functional theory calculations, we have identified and described the most probable structural and compositional configurations in rare-earth metal oxyhydride systems. Based on a large number of predicted compounds with different crystal structures and oxygen/hydrogen ratios, we pioneered in the development of a ternary phase diagram for the compositions Y−H−O. This allowed us to characterize the key role of oxygen in crystalline oxyhydrides, which is the leading component responsible for the stabilization of the multi-anion framework in ternary compounds.

We have shown that in certain cases off-center displacements of cations and anions must occur during condensation of an oxyhydride compound in order to gain a stable structure. This effect can lead to the breaking of the inversion symmetry of the crystal structure and cause macroscopic asymmetry of the charge density. Among all ternary oxyhydride compositions, we found that compositions in the form Ln_2H_4O (Ln = Y, La) can be stabilized in three noncentrosymmetric phases with monoclinic, orthorhombic and trigonal structures. Our predictions showed that the monoclinic and orthorhombic polar phases of Ln_2H_4O exhibit an outstanding piezoelectric response and can also provide high electromechanical characteristics.

We have demonstrated that the particular integration of oxygen atoms in the yttrium oxyhydride system may generate a new class of inorganic crystalline materials - metal hydroxyhydrides having a chemical composition $M_2H_3O(OH)$ (M = Y, Sc, La, and Gd). It was found that oxygen-induced specific transformations of the crystal structure lead to a change in the charge state of some hydrogen anions from negative H^- to positive H^+, forming thus proton sites in the hydroxyl groups. The strong localization of the charge at the hydrogen positions, caused by a special atomic ordering, is an important factor in stabilizing the chiral structural organization of the metal cations and anions forming the helical curves in the tetragonal structure $M_2H_3O(OH)$. The results of accurate DFT calculations have shown that this material, which has a totally chiral structure, can be used for the design and development of promising applications of nonlinear optics.

Based on the study of substitution effects in the polar oxyhydride system Ln_2H_4O we predicted a new family of multi-anion materials - $Ln_2OF_{2-x}Cl_xH_2$ (Ln = Y,La,Gd), which combines unique elastic characteristics with exceptional piezoelectric characteristics. This opens the way to the development of advanced energy harvesting devices that could merge the high piezoelectric power and elastic softness of PVDF-type piezopolymers on the one hand, and the thermal and high mechanical stability of solid piezoelectric ceramics on the other. Our estimates of energy harvesting efficiency showed that the power output of a piezoelectric

energy harvesting device using the Ln_2OClFH_2 system could be about 5-10 times that of commercially available PZT-5H ceramics, and about 3-4 times that of commercially available piezoelectric polymers.

To demonstrate how the combination of the effects of refraction, transmittance, and reflection together with the effect of internal interference of light waves can be used, we proposed two different prototypes of optical coatings in which oxyhydride thin films play a key role. (i) A low-emissivity coating model that is expected to block ultraviolet radiation and, to some extent, heating caused by infrared solar radiation. The model efficiency is that visible light can propagate with high transmittance (above 90%) and low reflectance (below 10%). (ii) A light-absorbing non-reflective coating model that is expected to exhibit high light absorption and low light reflection. Simulation results have shown that the proposed model can serve as a key component of broadband absorption coating. In the case of normal incidence, the system can absorb approximately 99.7% of incoming light over a wide wavelength range of $375 - 550$ nm; the highest absorption level, 99.98%, is reached at 395 nm.

The application of symmetry-based methods combined with accurate DFT calculations has helped us to predict and characterize materials of different chemical composition and structure. The key point of our approach is that modeling the lattice geometry of a three-dimensional crystal system does not require experimental knowledge of the spatial arrangement of atoms in the regular structure. The evolution of a specified structure is modeled by comparing the different crystallization pathways of substructures allowed in the hierarchy with respect to energy and stability conditions.

BIBLIOGRAPHY

[1] Aleksandr Pishtshev, **Evgenii Strugovshchikov**, and Smagul Karazhanov. "Conceptual Design of Yttrium Oxyhydrides: Phase Diagram, Structure, and Properties". In: *Cryst. Growth Des.* 19.5 (2019), pp. 2574–2582. DOI: https://doi.org/10.1021/acs.cgd.8b01596.

[2] Aleksandr Pishtshev and **Evgenii Strugovshchikov**. "Computational prediction of Ferro- and Piezoelectricity in Lead-free Oxyhydrides Ln_2H_4O (Ln = Y, La)". In: *Adv. Theory Simul.* 2.12 (2019), p. 1900144. DOI: https://doi.org/10.1002/adts.201900144.

[3] Aleksandr Pishtshev, **Evgenii Strugovshchikov**, and Smagul Karazhanov. "On prediction of a novel chiral material $Y_2H_3O(OH)$: A hydroxyhydride holding hydridic and protonic hydrogens". In: *Materials* 13.4 (2020), p. 994. DOI: https://doi.org/10.3390/ma13040994.

[4] Elbruz Murat Baba, Jose Montero, **Evgenii Strugovshchikov**, Esra Özkan Zayim, and Smagul Karazhanov. "Light-induced breathing in photochromic yttrium oxyhydrides". In: *Phys. Rev. Mater.* 4.2 (2020), p. 025201. DOI: https://doi.org/10.1103/PhysRevMaterials.4.025201.

[5] **Evgenii Strugovshchikov** and Aleksandr Pishtshev. "Exploring The Anion Chemical Space of $Ln_2OF_{2-x}Cl_xH_2$ (Ln=Y,La,Gd): A Model of Electroelastic Material with High Mechanical Sensitivity and Energy Harvesting". In: *Mater. Horiz* 8.2 (2021), pp. 577–588. DOI: https://doi.org/10.1039/D0MH01524E.

[6] **Evgenii Strugovshchikov**, Aleksandr Pishtshev, and Smagul Karazhanov. "Orthogonal chemistry in the design of rare-earth metal oxyhydrides". In: *Pure Appl. Chem.* -.- (2021), pp. -. DOI: https://doi.org/10.1515/pac-2021-0207.

[7] **Evgenii Strugovshchikov**, Aleksandr Pishtshev, and Smagul Karazhanov. "Theoretical design of effective multilayer optical coatings using oxyhydride thin films". In: *Phys. Status Solidi B* -.- (2021), pp. -. DOI: https://doi.org/10.1002/pssb.202100179.

[8] P. V. Borisyuk, E. V. Chubunova, Yu. Yu. Lebedinskii, E. V. Tkalya, O. S. Vasilyev, V. P. Yakovlev, **E. Strugovshchikov**, D. Mamedov, A. Pishtshev, and S. Zh. Karazhanov. "Experimental studies of thorium ion implantation from pulse laser plasma into thin silicon oxide layers". In: *Laser Physics Letters* 15.5 (2018), p. 056101. DOI: https://doi.org/10.1088/1612-202x/aaacf8.

[9] E.A. Vagapova, **E. Strugovshchikov**, E.O. Orlovskaya, A.S. Vanetsev, L. Dolgov, L. Puust, L.D. Iskhakova, U. Maeorg, A. Pishtshev, and Yu.V. Orlovskii. "Combined spectroscopic and DFT studies of local defect structures in beta-tricalcium phosphate doped with Nd(III)". In: *Journal of*

Alloys and Compounds 15.5 (2021), p. 160305. DOI: https://doi.org/10.1016/j.jallcom.2021.160305.

[10] "New, exotic materials: Getting oxygen into yttrium hydrides". In: *Research Outreach* 122 (May 2021). DOI: 10.32907/ro-122-1291164836. URL: https://doi.org/10.32907/ro-122-1291164836.

[11] Hiroshi Kageyama, Katsuro Hayashi, Kazuhiko Maeda, J. Attfield, Zenji Hiroi, James Rondinelli, and Kenneth Poeppelmeier. "Expanding frontiers in materials chemistry and physics with multiple anions". In: *Nat. Commun.* 9 (Feb. 2018), p. 772. DOI: 10.1038/s41467-018-02838-4.

[12] Fumitaka Takeiri and Hiroshi Kageyama. "Mixed-Anion Compounds: A New Trend in Solid State Chemistry". In: *Nihon Kessho Gakkaishi* 60 (Dec. 2018), pp. 240–245. DOI: 10.5940/jcrsj.60.240.

[13] David C. Fernández-Remolar. "Iron Oxides, Hydroxides and Oxy-hydroxides". In: *Encyclopedia of Astrobiology*. Ed. by Ricardo Amils, Muriel Gargaud, José Cernicharo Quintanilla, Henderson James Cleaves, William M. Irvine, Daniele Pinti, and Michel Viso. Berlin, Heidelberg: Springer Berlin Heidelberg, 2014, pp. 1–4. ISBN: 978-3-642-27833-4. DOI: 10.1007/978-3-642-27833-4_1714-3. URL: https://doi.org/10.1007/978-3-642-27833-4_1714-3.

[14] Vidal Barrón and José Torrent. "Iron, manganese and aluminium oxides and oxyhydroxides". In: *Minerals at the Nanoscale*. Mineralogical Society of Great Britain and Ireland, Jan. 2013. ISBN: 9780903056342. DOI: 10.1180/EMU-notes.14.9. URL: https://doi.org/10.1180/EMU-notes.14.9.

[15] Pa Ho Hsu. "Aluminum Hydroxides and Oxyhydroxides". In: *Minerals in Soil Environments*. John Wiley & Sons, Ltd, 1989, pp. 331–378. ISBN: 9780891188605. DOI: https://doi.org/10.2136/sssabookser1.2ed.c7. eprint: https://acsess.onlinelibrary.wiley.com/doi/pdf/10.2136/sssabookser1.2ed.c7. URL: https://acsess.onlinelibrary.wiley.com/doi/abs/10.2136/sssabookser1.2ed.c7.

[16] Manan Ahmed and Guo Xinxin. "A review of metal oxynitrides for photocatalysis". In: *Inorg. Chem. Front.* 3 (5 2016), pp. 578–590. DOI: 10.1039/C5QI00202H. URL: http://dx.doi.org/10.1039/C5QI00202H.

[17] Amparo Fuertes. "Metal oxynitrides as emerging materials with photocatalytic and electronic properties". In: *Mater. Horiz.* 2 (5 2015), pp. 453–461. DOI: 10.1039/C5MH00046G. URL: http://dx.doi.org/10.1039/C5MH00046G.

[18] Judith Oró-Solé, Ignasi Fina, Carlos Frontera, Jaume Gàzquez, Clemens Ritter, Marina Cunquero, Pablo Loza-Alvarez, Sergio Conejeros, Pere Alemany, Enric Canadell, Josep Fontcuberta, and Amparo Fuertes. "Engineering Polar Oxynitrides: Hexagonal Perovskite BaWON2". In: *Ange-*

wandte Chemie International Edition 59.42 (2020), pp. 18395–18399. DOI: https://doi.org/10.1002/anie.202006519. URL: https://onlinelibrary.wiley.com/doi/abs/10.1002/anie.202006519.

[19] Kallarackel T. Jacob, Viswanathan S. Saji, and Yoshio Waseda. "Lanthanum Oxyfluoride: Structure, Stability, and Ionic Conductivity". In: *Int. J. Appl. Ceram. Technol.* 3.4 (2006), pp. 312–321. DOI: 10.1111/j.1744-7402.2006.02086.x.

[20] E. Melnichenko, O. Gorbenko, N. Laptash, and S. Polyshchuk. "Solid transition metal oxyfluorides". In: *J. Fluorine Chem.* 45.1 (1989), p. 52. ISSN: 0022-1139. DOI: https://doi.org/10.1016/S0022-1139(00)84427-9. URL: http://www.sciencedirect.com/science/article/pii/S0022113900844279.

[21] Yoji Kobayashi, Mingliang Tian, Miharu Eguchi, and Thomas E Mallouk. "Ion-exchangeable, electronically conducting layered perovskite oxyfluorides". In: *J. Am. Chem. Soc.* 131.28 (July 2009), pp. 9849–9855. ISSN: 0002-7863. DOI: 10.1021/ja9040829. URL: https://doi.org/10.1021/ja9040829.

[22] A. W. Mann and D. J. M. Bevan. "The crystal structure of stoichiometric yttrium oxyfluoride, YOF". In: *Acta Crystallographica Section B* 26.12 (1970), pp. 2129–2131. DOI: 10.1107/S0567740870005496. eprint: https://onlinelibrary.wiley.com/doi/pdf/10.1107/S0567740870005496. URL: https://onlinelibrary.wiley.com/doi/abs/10.1107/S0567740870005496.

[23] Takafumi Yamamoto and Hiroshi Kageyama. "Hydride Reductions of Transition Metal Oxides". In: *Chem. Lett.* 42.9 (2013), pp. 946–953. DOI: 10.1246/cl.130581. eprint: https://doi.org/10.1246/cl.130581. URL: https://doi.org/10.1246/cl.130581.

[24] Yoji Kobayashi, Olivier Hernandez, Cédric Tassel, and Hiroshi Kageyama. "New chemistry of transition metal oxyhydrides". In: *Sci. Technol. Adv. Mater.* 18.1 (2017), pp. 905–918. DOI: 10.1080/14686996.2017.1394776. eprint: https://doi.org/10.1080/14686996.2017.1394776. URL: https://doi.org/10.1080/14686996.2017.1394776.

[25] T. Mongstad, C. Platzer-Björkman, S.Zh. Karazhanov, A. Holt, J.P. Maehlen, and B.C. Hauback. "Transparent yttrium hydride thin films prepared by reactive sputtering". In: *Journal of Alloys and Compounds* 509 (Sept. 2011), S812–S816. DOI: 10.1016/j.jallcom.2010.12.032. URL: https://doi.org/10.1016/j.jallcom.2010.12.032.

[26] Trygve Mongstad, Charlotte Platzer-Björkman, Jan Petter Maehlen, Lennard P.A. Mooij, Yevheniy Pivak, Bernard Dam, Erik S. Marstein, Bjørn C. Hauback, and Smagul Zh. Karazhanov. "A new thin film photochromic material: Oxygen-containing yttrium hydride". In: *Solar Energy Materials and Solar Cells* 95.12 (Dec. 2011), pp. 3596–3599. DOI: 10.1016/j.

solmat.2011.08.018. URL: https://doi.org/10.1016/j.solmat.2011.08.018.

[27] Trygve Mongstad, Annett Thøgersen, Aryasomayajula Subrahmanyam, and Smagul Karazhanov. "The electronic state of thin films of yttrium, yttrium hydrides and yttrium oxide". In: *Solar Energy Materials and Solar Cells* 128 (Sept. 2014), pp. 270–274. DOI: 10.1016/j.solmat.2014.05.037. URL: https://doi.org/10.1016/j.solmat.2014.05.037.

[28] V.N. Fokin, Yu.I. Malov, E.E. Fokina, S.L. Troitskaya, and S.P. Shilkin. "Investigation of interactions in the TiH_2-O_2 system". In: *Int. J. Hydrogen Energy* 20.5 (1995), pp. 387–389. DOI: https://doi.org/10.1016/0360-3199(94)00075-B. URL: http://www.sciencedirect.com/science/article/pii/036031999400075B.

[29] V.N. Fokin, Yu.I. Malov, E.E. Fokina, and S.P. Shilkin. "Study of the phase-forming features in the ZrH_2-O_2 system". In: *Int. J. Hydrogen Energy* 21 (Nov. 1996), pp. 969–973.

[30] V. N. Fokin, E. E. Fokina, and S. P. Shilkin. "Oxidation of Metal Hydrides with Molecular Oxygen". In: *Russ. J. Gen. Chem.* 74.4 (Apr. 2004), pp. 489–494. DOI: 10.1023/b:rugc.0000031845.00588.d0. URL: https://doi.org/10.1023/b:rugc.0000031845.00588.d0.

[31] Aleksandr Pishtshev and Smagul Zh. Karazhanov. "Role of oxygen in materials properties of yttrium trihydride". In: *Solid State Commun.* 194 (2014), pp. 39–42. ISSN: 0038-1098. DOI: https://doi.org/10.1016/j.ssc.2014.06.012. URL: http://www.sciencedirect.com/science/article/pii/S0038109814002671.

[32] K. Yoshimura, C. Langhammer, and B. Dam. "Metal hydrides for smart window and sensor applications". In: *MRS Bulletin* 38.6 (June 2013), pp. 495–503. DOI: 10.1557/mrs.2013.129. URL: https://doi.org/10.1557/mrs.2013.129.

[33] Kazuki Yoshimura. "Metal Hydrides for Smart-Window Applications". In: *Electrochromic Materials and Devices*. Wiley-VCH Verlag GmbH & Co. KGaA, July 2015, pp. 241–248. DOI: 10.1002/9783527679850.ch8. URL: https://doi.org/10.1002/9783527679850.ch8.

[34] G. Leftheriotis and P. Yianoulis. "Glazings and Coatings". In: *Reference Module in Earth Systems and Environmental Sciences*. Elsevier, 2020. DOI: 10.1016/b978-0-12-819727-1.00022-4. URL: https://doi.org/10.1016/b978-0-12-819727-1.00022-4.

[35] Elbruz Murat Baba, Jose Montero, Dmitrii Moldarev, Marcos Vinicius Moro, Max Wolff, Daniel Primetzhofer, Sabrina Sartori, Esra Zayim, and Smagul Karazhanov. "Preferential Orientation of Photochromic Gadolinium Oxyhydride Films". In: *Molecules* 25.14 (July 2020), p. 3181. DOI: 10.3390/molecules25143181. URL: https://doi.org/10.3390/molecules25143181.

[36] Chang Chuan You, Trygve Mongstad, Jan Petter Maehlen, and Smagul Karazhanov. “Dynamic reactive sputtering of photochromic yttrium hydride thin films”. In: *Solar Energy Materials and Solar Cells* 143 (Dec. 2015), pp. 623–626. DOI: 10.1016/j.solmat.2014.08.016. URL: https://doi.org/10.1016/j.solmat.2014.08.016.

[37] Chang Chuan You, Trygve Mongstad, Erik Stensrud Marstein, and Smagul Zh. Karazhanov. “The dependence of structural, electrical and optical properties on the composition of photochromic yttrium oxyhydride thin films”. In: *Materialia* 6 (June 2019), p. 100307. DOI: 10.1016/j.mtla.2019.100307. URL: https://doi.org/10.1016/j.mtla.2019.100307.

[38] Dmitrii Moldarev, Marcos V. Moro, Chang C. You, Elbruz M. Baba, Smagul Zh. Karazhanov, Max Wolff, and Daniel Primetzhofer. “Yttrium oxyhydrides for photochromic applications: Correlating composition and optical response”. In: *Physical Review Materials* 2.11 (Nov. 2018). DOI: 10.1103/physrevmaterials.2.115203. URL: https://doi.org/10.1103/physrevmaterials.2.115203.

[39] Dmitrii Moldarev, Daniel Primetzhofer, Chang Chuan You, Smagul Zh. Karazhanov, Jose Montero, Fredrik Martinsen, Trygve Mongstad, Erik S. Marstein, and Max Wolff. “Composition of photochromic oxygen-containing yttrium hydride films”. In: *Solar Energy Materials and Solar Cells* 177 (Apr. 2018), pp. 66–69. DOI: 10.1016/j.solmat.2017.05.052. URL: https://doi.org/10.1016/j.solmat.2017.05.052.

[40] M.V. Moro, D. Moldarev, C.C. You, E.M. Baba, S.Zh. Karazhanov, M. Wolff, and D. Primetzhofer. “In-situ composition analysis of photochromic yttrium oxy-hydride thin films under light illumination”. In: *Solar Energy Materials and Solar Cells* 201 (Oct. 2019), p. 110119. DOI: 10.1016/j.solmat.2019.110119. URL: https://doi.org/10.1016/j.solmat.2019.110119.

[41] Chang Chuan You, Dmitrii Moldarev, Trygve Mongstad, Daniel Primetzhofer, Max Wolff, Erik Stensrud Marstein, and Smagul Zh. Karazhanov. “Enhanced photochromic response in oxygen-containing yttrium hydride thin films transformed by an oxidation process”. In: *Solar Energy Materials and Solar Cells* 166 (July 2017), pp. 185–189. DOI: 10.1016/j.solmat.2017.03.023. URL: https://doi.org/10.1016/j.solmat.2017.03.023.

[42] Jan Petter Maehlen, Trygve T. Mongstad, Chang Chuan You, and Smagul Karazhanov. “Lattice contraction in photochromic yttrium hydride”. In: *Journal of Alloys and Compounds* 580 (Dec. 2013), S119–S121. DOI: 10.1016/j.jallcom.2013.03.151. URL: https://doi.org/10.1016/j.jallcom.2013.03.151.

[43] Chang Chuan You, Trygve Mongstad, Jan Petter Maehlen, and Smagul Karazhanov. "Engineering of the band gap and optical properties of thin films of yttrium hydride". In: *Applied Physics Letters* 105.3 (July 2014), p. 031910. DOI: 10.1063/1.4891175. URL: https://doi.org/10.1063/1.4891175.

[44] D. Moldarev, M. Wolff, E.M. Baba, M.V. Moro, C.C. You, D. Primetzhofer, and S.Zh. Karazhanov. "Photochromic properties of yttrium oxyhydride thin films: Surface versus bulk effect". In: *Materialia* 11 (June 2020), p. 100706. DOI: 10.1016/j.mtla.2020.100706. URL: https://doi.org/10.1016/j.mtla.2020.100706.

[45] José Montero and Smagul Z. Karazhanov. "Spectroscopic Ellipsometry and Microstructure Characterization of Photochromic Oxygen-Containing Yttrium Hydride Thin Films". In: *physica status solidi (a)* 215.19 (Mar. 2018), p. 1701039. DOI: 10.1002/pssa.201701039. URL: https://doi.org/10.1002/pssa.201701039.

[46] Francesca Ercole, Thomas P. Davis, and Richard A. Evans. "Photo-responsive systems and biomaterials: photochromic polymers, light-triggered self-assembly, surface modification, fluorescence modulation and beyond". In: *Polym. Chem.* 1.1 (2010), pp. 37–54. DOI: 10.1039/b9py00300b. URL: https://doi.org/10.1039/b9py00300b.

[47] "The nature of the chemical bond and the structure of molecules and crystals, by Linus Pauling. 2nd Edition. xvi + 450 pages. Cornell University Press, Ithaca, N. Y., 1940." In: *Journal of the American Pharmaceutical Association (Scientific ed.)* 30.1 (Jan. 1941), p. 30. DOI: 10.1002/jps.3030300111. URL: https://doi.org/10.1002/jps.3030300111.

[48] R. D. Shannon. "Revised effective ionic radii and systematic studies of interatomic distances in halides and chalcogenides". In: *Acta Crystallographica Section A* 32.5 (Sept. 1976), pp. 751–767. DOI: 10.1107/s0567739476001551.

[49] C. Blondel, P. Cacciani, C. Delsart, and R. Trainham. "High-resolution determination of the electron affinity of fluorine and bromine using crossed ion and laser beams". In: *Physical Review A* 40.7 (Oct. 1989), pp. 3698–3701. DOI: 10.1103/physreva.40.3698. URL: https://doi.org/10.1103/physreva.40.3698.

[50] K. R. Lykke, K. K. Murray, and W. C. Lineberger. "Threshold photodetachment ofH-". In: *Physical Review A* 43.11 (June 1991), pp. 6104–6107. DOI: 10.1103/physreva.43.6104. URL: https://doi.org/10.1103/physreva.43.6104.

[51] W. Chaibi, R. J. Peláez, C. Blondel, C. Drag, and C. Delsart. "Effect of a magnetic field in photodetachment microscopy". In: *The European Physical Journal D* 58.1 (Apr. 2010), pp. 29–37. DOI: 10.1140/epjd/

e2010-00086-7. URL: https://doi.org/10.1140/epjd/e2010-00086-7.

[52] Katsuro Hayashi, Peter V. Sushko, Yasuhiro Hashimoto, Alexander L. Shluger, and Hideo Hosono. "Hydride ions in oxide hosts hidden by hydroxide ions". In: *Nature Communications* 5.1 (Mar. 2014). DOI: 10.1038/ncomms4515. URL: https://doi.org/10.1038/ncomms4515.

[53] V SHEMET, A POMYTKIN, V LAVRENKO, and V RATUSHNAYA. "Decomposition of metal hydrides in low temperatures and in high-temperature oxidation". In: *International Journal of Hydrogen Energy* 18.6 (June 1993), pp. 511–516. DOI: 10.1016/0360-3199(93)90008-x. URL: https://doi.org/10.1016/0360-3199(93)90008-x.

[54] Hugo Ricardo Zschommler Sandim, Bruno Vieira Morante, and Paulo Atsushi Suzuki. "Kinetics of thermal decomposition of titanium hydride powder using in situ high-temperature X-ray diffraction (HTXRD)". In: *Materials Research* 8.3 (Sept. 2005), pp. 293–297. DOI: 10.1590/s1516-14392005000300012. URL: https://doi.org/10.1590/s1516-14392005000300012.

[55] Young Jun KWAK, Hye Ryoung PARK, and Myoung Youp SONG. "Analysis of the Metal hydride Decomposition Temperatures of Zn(BH4)2 – MgH2 – Tm (Tm = Ni, Ti or Fe) Using a Sievert's Type Volumetric Apparatus". In: *Materials Science* 23.1 (Feb. 2017). DOI: 10.5755/j01.ms.23.1.14270. URL: https://doi.org/10.5755/j01.ms.23.1.14270.

[56] Th. Becker, St. Hövel, M. Kunat, Ch. Boas, U. Burghaus, and Ch. Wöll. "Interaction of hydrogen with metal oxides: the case of the polar ZnO(0001) surface". In: *Surface Science* 486.3 (July 2001), pp. L502–L506. DOI: 10.1016/s0039-6028(01)01120-7. URL: https://doi.org/10.1016/s0039-6028(01)01120-7.

[57] Xingqun Zheng, Li Li, Mingming Deng, Jing Li, Wei Ding, Yao Nie, and Zidong Wei. "Understanding the effect of interfacial interaction on metal/metal oxide electrocatalysts for hydrogen evolution and hydrogen oxidation reactions on the basis of first-principles calculations". In: *Catalysis Science & Technology* 10.14 (2020), pp. 4743–4751. DOI: 10.1039/d0cy00960a. URL: https://doi.org/10.1039/d0cy00960a.

[58] Takafumi Yamamoto and Hiroshi Kageyama. "Hydride Reductions of Transition Metal Oxides". In: *Chemistry Letters* 42.9 (2013), pp. 946–953. DOI: 10.1246/cl.130581. eprint: https://doi.org/10.1246/cl.130581. URL: https://doi.org/10.1246/cl.130581.

[59] Genki Kobayashi, Yoyo Hinuma, Shinji Matsuoka, Akihiro Watanabe, Muhammad Iqbal, Masaaki Hirayama, Masao Yonemura, Takashi Kamiyama, Isao Tanaka, and Ryoji Kanno. "Pure H– conduction in oxyhydrides". In: *Science* 351.6279 (2016), pp. 1314–1317. ISSN: 0036-8075. DOI: 10.1126/science.aac9185. eprint: https://science.sciencemag.

org/content/351/6279/1314.full.pdf. URL: https://science.sciencemag.org/content/351/6279/1314.

[60] Yoji Kobayashi, Olivier Hernandez, Cédric Tassel, and Hiroshi Kageyama. "New chemistry of transition metal oxyhydrides". In: *Science and Technology of Advanced Materials* 18.1 (2017). PMID: 29383042, pp. 905–918. DOI: 10.1080/14686996.2017.1394776. eprint: https://doi.org/10.1080/14686996.2017.1394776. URL: https://doi.org/10.1080/14686996.2017.1394776.

[61] Yoji Kobayashi et al. "An oxyhydride of BaTiO3 exhibiting hydride exchange and electronic conductivity". In: *Nature Materials* 11.6 (June 2012), pp. 507–511. ISSN: 1476-4660. DOI: 10.1038/nmat3302. URL: https://doi.org/10.1038/nmat3302.

[62] Tatsunori Sakaguchi et al. "Oxyhydrides of (Ca,Sr,Ba)TiO_3 Perovskite Solid Solutions". In: *Inorganic Chemistry* 51.21 (2012). PMID: 23082857, pp. 11371–11376. DOI: 10.1021/ic300859n. eprint: https://doi.org/10.1021/ic300859n. URL: https://doi.org/10.1021/ic300859n.

[63] Takafumi Yamamoto, Ryuta Yoshii, Guillaume Bouilly, Yoji Kobayashi, Koji Fujita, Yoshiro Kususe, Yoshitaka Matsushita, Katsuhisa Tanaka, and Hiroshi Kageyama. "An Antiferro-to-Ferromagnetic Transition in EuTiO3–xHx Induced by Hydride Substitution". In: *Inorganic Chemistry* 54.4 (2015). PMID: 25594721, pp. 1501–1507. DOI: 10.1021/ic502486e. eprint: https://doi.org/10.1021/ic502486e. URL: https://doi.org/10.1021/ic502486e.

[64] C. A. Bridges, F. Fernandez-Alonso, J. P. Goff, and M. J. Rosseinsky. "Observation of Hydride Mobility in the Transition-Metal Oxide Hydride LaSrCoO3H0.7". In: *Advanced Materials* 18.24 (Dec. 2006), pp. 3304–3308. DOI: 10.1002/adma.200601266. URL: https://doi.org/10.1002/adma.200601266.

[65] Fabio Denis Romero, Alice Leach, Johannes S. Moller, Francesca Foronda, Stephen J. Blundell, and Michael A. Hayward. "Strontium Vanadium Oxide–Hydrides: "Square-Planar" Two-Electron Phases". In: *Angewandte Chemie International Edition* 53.29 (2014), pp. 7556–7559. DOI: https://doi.org/10.1002/anie.201403536. eprint: https://onlinelibrary.wiley.com/doi/pdf/10.1002/anie.201403536. URL: https://onlinelibrary.wiley.com/doi/abs/10.1002/anie.201403536.

[66] Cedric Tassel, Yoshinori Goto, Daichi Watabe, Ya Tang, Honcheng Lu, Yoshinori Kuno, Fumitaka Takeiri, Takafumi Yamamoto, Craig M. Brown, James Hester, Yoji Kobayashi, and Hiroshi Kageyama. "High-Pressure Synthesis of Manganese Oxyhydride with Partial Anion Order". In: *Angewandte Chemie* 128.33 (June 2016), pp. 9819–9822. DOI: 10.1002/ange.201605123. URL: https://doi.org/10.1002/ange.201605123.

[67] Joonho Bang, Satoru Matsuishi, Haruhiro Hiraka, Fumika Fujisaki, Toshiya Otomo, Sachiko Maki, Jun-ichi Yamaura, Reiji Kumai, Youichi Murakami, and Hideo Hosono. "Hydrogen Ordering and New Polymorph of Layered Perovskite Oxyhydrides: Sr2VO4–xHx". In: *Journal of the American Chemical Society* 136.20 (May 2014), pp. 7221–7224. DOI: 10.1021/ja502277r. URL: https://doi.org/10.1021/ja502277r.

[68] Cédric Tassel, Yoshihiro Goto, Yoshinori Kuno, James Hester, Mark Green, Yoji Kobayashi, and Hiroshi Kageyama. "Direct Synthesis of Chromium Perovskite Oxyhydride with a High Magnetic-Transition Temperature". In: *Angewandte Chemie International Edition* 53.39 (Aug. 2014), pp. 10377–10380. DOI: 10.1002/anie.201405453. URL: https://doi.org/10.1002/anie.201405453.

[69] José Montero, Fredrik A. Martinsen, Martynas Lelis, Smagul Zh. Karazhanov, Bjørn C. Hauback, and Erik S. Marstein. "Preparation of yttrium hydride-based photochromic films by reactive magnetron sputtering". In: *Solar Energy Materials and Solar Cells* 177 (2018). SI:IME-12 Delft, pp. 106–109. ISSN: 0927-0248. DOI: https://doi.org/10.1016/j.solmat.2017.02.001.

[70] Chang Chuan You and Smagul Zh. Karazhanov. "Effect of temperature and illumination conditions on the photochromic performance of yttrium oxyhydride thin films". In: *Journal of Applied Physics* 128.1 (July 2020), p. 013106. DOI: 10.1063/5.0010132. URL: https://doi.org/10.1063/5.0010132.

[71] C. Vinod Chandran, Herman Schreuders, Bernard Dam, Johannes W. G. Janssen, Jacob Bart, Arno P. M. Kentgens, and P. Jan M. van Bentum. "Solid-State NMR Studies of the Photochromic Effects of Thin Films of Oxygen-Containing Yttrium Hydride". In: *The Journal of Physical Chemistry C* 118.40 (Sept. 2014), pp. 22935–22942. DOI: 10.1021/jp507248c. URL: https://doi.org/10.1021/jp507248c.

[72] F. Nafezarefi, H. Schreuders, B. Dam, and S. Cornelius. "Photochromism of rare-earth metal-oxy-hydrides". In: *Applied Physics Letters* 111.10 (Sept. 2017), p. 103903. DOI: 10.1063/1.4995081. URL: https://doi.org/10.1063/1.4995081.

[73] Nicolas Zapp, Henry Auer, and Holger Kohlmann. "YHO, an Air-Stable Ionic Hydride". In: *Inorganic Chemistry* 58.21 (Oct. 2019), pp. 14635–14641. DOI: 10.1021/acs.inorgchem.9b02308. URL: https://doi.org/10.1021/acs.inorgchem.9b02308.

[74] A. Miniotas, B. Hjörvarsson, L. Douysset, and P. Nostell. "Gigantic resistivity and band gap changes in GdO_yH_x thin films". In: *Applied Physics Letters* 76.15 (Apr. 2000), pp. 2056–2058. DOI: 10.1063/1.126253. URL: https://doi.org/10.1063/1.126253.

[75] A Fujimori and L Schlapbach. “Electronic structure of yttrium hydride studied by X-ray photoemission spectroscopy”. In: *Journal of Physics C: Solid State Physics* 17.2 (Jan. 1984), pp. 341–351. DOI: 10.1088/0022-3719/17/2/021. URL: https://doi.org/10.1088/0022-3719/17/2/021.

[76] M.P. Plokker, S.W.H. Eijt, F. Naziris, H. Schut, F. Nafezarefi, H. Schreuders, S. Cornelius, and B. Dam. “Electronic structure and vacancy formation in photochromic yttrium oxy-hydride thin films studied by positron annihilation”. In: *Solar Energy Materials and Solar Cells* 177 (Apr. 2018), pp. 97–105. DOI: 10.1016/j.solmat.2017.03.011. URL: https://doi.org/10.1016/j.solmat.2017.03.011.

[77] WILLIAM J. TROPF and MICHAEL E. THOMAS. “Yttrium Oxide (Y2O3)”. In: *Handbook of Optical Constants of Solids*. Elsevier, 1998, pp. 1079–1096. DOI: 10.1016/b978-0-08-055630-7.50065-1. URL: https://doi.org/10.1016/b978-0-08-055630-7.50065-1.

[78] Frederick Wooten. “Chapter 4 - FREE-ELECTRON METALS”. In: *Optical Properties of Solids*. Ed. by Frederick Wooten. Academic Press, 1972, pp. 85–107. ISBN: 978-0-12-763450-0. DOI: https://doi.org/10.1016/B978-0-12-763450-0.50009-X.

[79] A.M. Fox and D.P.A.M. Fox. *Optical Properties of Solids*. Oxford master series in condensed matter physics. Oxford University Press, 2001. ISBN: 9780198506126. URL: https://books.google.ee/books?id=-5bVBbAoaGoC.

[80] Jan Mistrik, Safa Kasap, Harry E. Ruda, Cyril Koughia, and Jai Singh. “Optical Properties of Electronic Materials: Fundamentals and Characterization”. In: *Springer Handbook of Electronic and Photonic Materials*. Ed. by Safa Kasap and Peter Capper. Cham: Springer International Publishing, 2017, pp. 1–1. ISBN: 978-3-319-48933-9. DOI: 10.1007/978-3-319-48933-9_3. URL: https://doi.org/10.1007/978-3-319-48933-9_3.

[81] Jasprit Singh. *Electronic and Optoelectronic Properties of Semiconductor Structures*. Cambridge University Press, Jan. 2003. DOI: 10.1017/cbo9780511805745.

[82] M. Cardona and P.Y. Yu. “Optical Properties of Semiconductors”. In: *Comprehensive Semiconductor Science and Technology*. Elsevier, 2011, pp. 125–195. DOI: 10.1016/b978-0-44-453153-7.00073-0. URL: https://doi.org/10.1016/b978-0-44-453153-7.00073-0.

[83] A. T. M. van Gogh, D. G. Nagengast, E. S. Kooij, N. J. Koeman, J. H. Rector, R. Griessen, C. F. J. Flipse, and R. J. J. G. A. M. Smeets. “Structural, electrical, and optical properties ofLa1-zYzHxswitchable mirrors”. In: *Physical Review B* 63.19 (Apr. 2001). DOI: 10.1103/physrevb.63.195105. URL: https://doi.org/10.1103/physrevb.63.195105.

[84] Yong-Nian Xu, Zhong-quan Gu, and W. Y. Ching. “Electronic, structural, and optical properties of crystalline yttria”. In: *Physical Review B* 56.23 (Dec. 1997), pp. 14993–15000. DOI: 10.1103/physrevb.56.14993. URL: https://doi.org/10.1103/physrevb.56.14993.

[85] M. Irie. “Photochromism: Memories and SwitchesIntroduction”. In: *Chemical Reviews* 100.5 (May 2000), pp. 1683–1684. DOI: 10.1021/cr9800681. URL: https://doi.org/10.1021/cr9800681.

[86] Richard A. Evans, Tracey L. Hanley, Melissa A. Skidmore, Thomas P. Davis, Georgina K. Such, Lachlan H. Yee, Graham E. Ball, and David A. Lewis. “The generic enhancement of photochromic dye switching speeds in a rigid polymer matrix”. In: *Nature Materials* 4.3 (Feb. 2005), pp. 249–253. DOI: 10.1038/nmat1326. URL: https://doi.org/10.1038/nmat1326.

[87] D.R. Arnold, N.C. Baird, J.R. Bolton, J.C.D. Brand, P.W.M. Jacobs, P. de Mayo, and W.R. Ware. “PHOTOCHROMISM”. In: *Photochemistry*. Elsevier, 1974, pp. 238–261. DOI: 10.1016/b978-0-12-063350-0.50013-4. URL: https://doi.org/10.1016/b978-0-12-063350-0.50013-4.

[88] Ayako Ohmura, Akihiko Machida, Tetsu Watanuki, Katsutoshi Aoki, Satoshi Nakano, and K. Takemura. “Photochromism in yttrium hydride”. In: *Applied Physics Letters* 91.15 (Oct. 2007), p. 151904. DOI: 10.1063/1.2794755. URL: https://doi.org/10.1063/1.2794755.

[89] J. Friedel. “Crystallography and crystal defectsby A. Kelly and G. W. Groves”. In: *Journal of Applied Crystallography* 9.3 (June 1976), pp. 262–262. DOI: 10.1107/s0021889876011308. URL: https://doi.org/10.1107/s0021889876011308.

[90] J. H. Robertson. “Crystallography: an introduction for earth science (and other solid state) students by E. J. W. Whittaker”. In: *Acta Crystallographica Section B Structural Crystallography and Crystal Chemistry* 38.7 (July 1982), pp. 2098–2098. DOI: 10.1107/s0567740882012928. URL: https://doi.org/10.1107/s0567740882012928.

[91] Martin Weller. *Inorganic chemistry*. Oxford: Oxford University Press, 2018. ISBN: 9780198768128.

[92] Neil Ashcroft. *Solid state physics*. New York: Holt, Rinehart and Winston, 1976. ISBN: 0030493463.

[93] Robert Carter. *Molecular symmetry and group theory*. New York: J. Wiley, 1998. ISBN: 978-0-471-14955-2.

[94] E.S. Fedorov. “Symmetry of crystals”. In: *Journal of Molecular Structure* 18.1 (Sept. 1973), p. 152. DOI: 10.1016/0022-2860(73)80092-4. URL: https://doi.org/10.1016/0022-2860(73)80092-4.

[95] A. Gadolin. “Abhandlung über die herleitung aller krystallographischer systeme”. In: *Zeitschrift für Krystallographie und Mineralogie* 1.1 (Sept. 1896), p. 114.

[96] Axel Gadolin. “Eine einfache Methode zur Bestimmung des specifischen Gewichtes der Mineralien”. In: *Annalen der Physik und Chemie* 182.2 (1859), pp. 213–225. DOI: 10.1002/andp.18591820204. URL: https://doi.org/10.1002/andp.18591820204.

[97] J. J. Burckhardt. “Der Briefwechsel von E. S. von Fedorow und A. Schoenflies, 1889-1908”. In: *Archive for History of Exact Sciences* 7.2 (1971), pp. 91–141. DOI: 10.1007/bf00411807. URL: https://doi.org/10.1007/bf00411807.

[98] William Barlow. “I. Ueber die geometrischen Eigenschaften homogener starrer Structuren und ihre Anwendung auf Krystalle.” In: *Zeitschrift für Kristallographie - Crystalline Materials* 23.1-6 (Jan. 1894), pp. 1–63. DOI: 10.1524/zkri.1894.23.1.1. URL: https://doi.org/10.1524/zkri.1894.23.1.1.

[99] Ludwig Bieberbach. “Über die Bewegungsgruppen der Euklidischen Räume (Zweite Abhandlung.) Die Gruppen mit einem endlichen Fundamentalbereich”. In: *Mathematische Annalen* 72.3 (Sept. 1912), pp. 400–412. DOI: 10.1007/bf01456724. URL: https://doi.org/10.1007/bf01456724.

[100] J. J. Burckhardt. “Zur Geschichte der Entdeckung der 230 Raumgruppen”. In: *Archive for History of Exact Sciences* 4.3 (1967), pp. 235–246. DOI: 10.1007/bf00412962. URL: https://doi.org/10.1007/bf00412962.

[101] Peter Paufler and Stanislav K. Filatov. “E. S. Fedorov Promoting the Russian-German Scientific Interrelationship”. In: *Minerals* 10.2 (Feb. 2020), p. 181. DOI: 10.3390/min10020181. URL: https://doi.org/10.3390/min10020181.

[102] S. Ivantchev, E. Kroumova, G. Madariaga, J. M. Pérez-Mato, and M. I. Aroyo. “*SUBGROUPGRAPH*: a computer program for analysis of group–subgroup relations between space groups”. In: *J. Appl. Crystallogr.* 33.4 (2000), pp. 1190–1191. DOI: 10.1107/S0021889800007135.

[103] E. Kroumova, M. I. Aroyo, J. M. Pérez-Mato, C. Capillas, S. Ivantchev, and H. Wondratschek. “Bilbao Crystallographic Server I: Databases and crystallographic computing programs”. In: *Phase Transitions* 76 (1-2 2003), pp. 155–170. DOI: doi:10.1080/0141159031000076110.

[104] M.I. Aroyo, J.M. Pérez-Mato, D. Orobengoa, E.S. Tasci, G. de la Flor, and A. Kirov. “Crystallography online: Bilbao Crystallographic Server”. In: *Bulg. Chem. Commun.* 43.2 (2011), pp. 183–197.

[105] M.I. Aroyo, J.M. Pérez-Mato, C. Capillas, E. Kroumova, S. Ivantchev, G. Madariaga, A. Kirov, and H. Wondratschek. “Bilbao Crystallographic Server I: Databases and crystallographic computing programs”. In: *Z. Krist.* 221.1 (2006), pp. 15–27.

[106] Mois I. Aroyo, Asen Kirov, Cesar Capillas, J. M. Pérez-Mato, and Hans Wondratschek. “Bilbao Crystallographic Server. II. Representations of crystallographic point groups and space groups”. In: *Acta Cryst.* A62.2 (2006), pp. 115–128. DOI: 10.1107/S0108767305040286.

[107] Koichi Momma and Fujio Izumi. “VESTA 3for three-dimensional visualization of crystal, volumetric and morphology data”. In: *Journal of Applied Crystallography* 44.6 (Oct. 2011), pp. 1272–1276. DOI: 10.1107/s0021889811038970.

[108] Fujio Izumi and Koichi Momma. “Three-Dimensional Visualization in Powder Diffraction”. In: *Solid State Phenomena* 130 (Dec. 2007), pp. 15–20. DOI: 10.4028/www.scientific.net/ssp.130.15. URL: https://doi.org/10.4028/www.scientific.net/ssp.130.15.

[109] Koichi Momma and Fujio Izumi. “VESTA: a three-dimensional visualization system for electronic and structural analysis”. In: *Journal of Applied Crystallography* 41.3 (May 2008), pp. 653–658. DOI: 10.1107/s0021889808012016.

[110] Fujio Izumi. “Structure Analysis by Powder Diffraction with the RIETAN-FP-VENUS System and External Programs —1. The RIETAN-FP-VENUS System and Integrated Assistance Environment—”. In: *Materia Japan* 56.6 (2017), pp. 393–396. DOI: 10.2320/materia.56.393. URL: https://doi.org/10.2320/materia.56.393.

[111] G. Kresse and J. Hafner. “Ab initiomolecular dynamics for open-shell transition metals”. In: *Physical Review B* 48.17 (Nov. 1993), pp. 13115–13118. DOI: 10.1103/physrevb.48.13115. URL: https://doi.org/10.1103/physrevb.48.13115.

[112] G. Kresse and J. Hafner. “Ab initiomolecular dynamics for liquid metals”. In: *Physical Review B* 47.1 (Jan. 1993), pp. 558–561. DOI: 10.1103/physrevb.47.558. URL: https://doi.org/10.1103/physrevb.47.558.

[113] G. Kresse and J. Hafner. “Ab initiomolecular-dynamics simulation of the liquid-metal–amorphous-semiconductor transition in germanium”. In: *Physical Review B* 49.20 (May 1994), pp. 14251–14269. DOI: 10.1103/physrevb.49.14251. URL: https://doi.org/10.1103/physrevb.49.14251.

[114] G. Kresse and J. Furthmüller. “Efficient iterative schemes forab initiototal-energy calculations using a plane-wave basis set”. In: *Physical Review B* 54.16 (Oct. 1996), pp. 11169–11186. DOI: 10.1103/physrevb.54.11169. URL: https://doi.org/10.1103/physrevb.54.11169.

[115] G. Kresse and J. Furthmüller. “Efficiency of ab-initio total energy calculations for metals and semiconductors using a plane-wave basis set”. In: *Computational Materials Science* 6.1 (July 1996), pp. 15–50. DOI:

10.1016/0927-0256(96)00008-0. URL: https://doi.org/10.1016/0927-0256(96)00008-0.

[116] Jochen Heyd, Gustavo E. Scuseria, and Matthias Ernzerhof. "Hybrid functionals based on a screened Coulomb potential". In: *J. Chem. Phys.* 118.18 (2003), pp. 8207–8215. DOI: 10.1063/1.1564060. eprint: https://doi.org/10.1063/1.1564060. URL: https://doi.org/10.1063/1.1564060.

[117] Aliaksandr V. Krukau, Oleg A. Vydrov, Artur F. Izmaylov, and Gustavo E. Scuseria. "Influence of the exchange screening parameter on the performance of screened hybrid functionals". In: *J. Chem. Phys.* 125.22 (2006), p. 224106. DOI: 10.1063/1.2404663. eprint: https://doi.org/10.1063/1.2404663. URL: https://doi.org/10.1063/1.2404663.

[118] Thomas M. Henderson, Joachim Paier, and Gustavo E. Scuseria. "Accurate treatment of solids with the HSE screened hybrid". In: *Phys. Status Solidi B* 248.4 (2011), pp. 767–774. DOI: 10.1002/pssb.201046303. eprint: https://onlinelibrary.wiley.com/doi/pdf/10.1002/pssb.201046303. URL: https://onlinelibrary.wiley.com/doi/abs/10.1002/pssb.201046303.

[119] Audrius Alkauskas, Peter Broqvist, Fabien Devynck, and Alfredo Pasquarello. "Band Offsets at Semiconductor-Oxide Interfaces from Hybrid Density-Functional Calculations". In: *Phys. Rev. Lett.* 101 (10 Sept. 2008), p. 106802. DOI: 10.1103/PhysRevLett.101.106802. URL: https://link.aps.org/doi/10.1103/PhysRevLett.101.106802.

[120] Audrius Alkauskas, Peter Broqvist, and Alfredo Pasquarello. "Defect levels through hybrid density functionals: Insights and applications". In: *Phys. Status Solidi B* 248.4 (2011), pp. 775–789. DOI: 10.1002/pssb.201046195. eprint: https://onlinelibrary.wiley.com/doi/pdf/10.1002/pssb.201046195. URL: https://onlinelibrary.wiley.com/doi/abs/10.1002/pssb.201046195.

[121] Miguel A. L. Marques, Julien Vidal, Micael J. T. Oliveira, Lucia Reining, and Silvana Botti. "Density-based mixing parameter for hybrid functionals". In: *Phys. Rev. B* 83 (3 Jan. 2011), p. 035119. DOI: 10.1103/PhysRevB.83.035119. URL: https://link.aps.org/doi/10.1103/PhysRevB.83.035119.

[122] Jiangang He and Cesare Franchini. "Screened hybrid functional applied to $3d^0 \rightarrow 3d^8$ transition-metal perovskites $LaMO_3$ (M = Sc–Cu): Influence of the exchange mixing parameter on the structural, electronic, and magnetic properties". In: *Phys. Rev. B* 86 (23 Dec. 2012), p. 235117. DOI: 10.1103/PhysRevB.86.235117. URL: https://link.aps.org/doi/10.1103/PhysRevB.86.235117.

[123] Lars Hedin. "New Method for Calculating the One-Particle Green's Function with Application to the Electron-Gas Problem". In: *Physical Review*

139.3A (Aug. 1965), A796–A823. DOI: 10.1103/physrev.139.a796. URL: https://doi.org/10.1103/physrev.139.a796.

[124] Julien Vidal, Silvana Botti, Pär Olsson, Jean-Fran çois Guillemoles, and Lucia Reining. "Strong Interplay between Structure and Electronic Properties in CuIn(S,Se_2): A First-Principles Study". In: *Phys. Rev. Lett.* 104 (5 Feb. 2010), p. 056401. DOI: 10.1103/PhysRevLett.104.056401. URL: https://link.aps.org/doi/10.1103/PhysRevLett.104.056401.

[125] Silvana Botti and Julien Vidal. "Energy Generation: Solar Energy". In: *Computational Approaches to Energy Materials*. John Wiley & Sons Ltd, Apr. 2013, pp. 29–69. DOI: 10.1002/9781118551462.ch2. URL: https://doi.org/10.1002/9781118551462.ch2.

[126] P. E. Blöchl. "Projector augmented-wave method". In: *Physical Review B* 50.24 (Dec. 1994), pp. 17953–17979. DOI: 10.1103/physrevb.50.17953. URL: https://doi.org/10.1103/physrevb.50.17953.

[127] W. Cochran and R.A. Cowley. "Dielectric constants and lattice vibrations". In: *Journal of Physics and Chemistry of Solids* 23.5 (May 1962), pp. 447–450. DOI: 10.1016/0022-3697(62)90084-7. URL: https://doi.org/10.1016/0022-3697(62)90084-7.

[128] R.A. Cowley. "Structural phase transitions I. Landau theory". In: *Advances in Physics* 29.1 (Feb. 1980), pp. 1–110. DOI: 10.1080/00018738000101346. URL: https://doi.org/10.1080/00018738000101346.

[129] R. A. Cowley. "Acoustic phonon instabilities and structural phase transitions". In: *Physical Review B* 13.11 (June 1976), pp. 4877–4885. DOI: 10.1103/physrevb.13.4877. URL: https://doi.org/10.1103/physrevb.13.4877.

[130] J.F. Nye and P.P.L.J.F. Nye. *Physical Properties of Crystals: Their Representation by Tensors and Matrices*. Oxford science publications. Clarendon Press, 1985. ISBN: 9780198511656. URL: https://books.google.es/books?id=ugwql-uVB44C.

[131] Romain Gaillac, Pluton Pullumbi, and François-Xavier Coudert. "ELATE: an open-source online application for analysis and visualization of elastic tensors". In: *Journal of Physics: Condensed Matter* 28.27 (May 2016), p. 275201. DOI: 10.1088/0953-8984/28/27/275201. URL: https://doi.org/10.1088/0953-8984/28/27/275201.

[132] Woldemar Voigt. *Lehrbuch der Kristallphysik*. Vieweg+Teubner Verlag, 1966. DOI: 10.1007/978-3-663-15884-4. URL: https://doi.org/10.1007/978-3-663-15884-4.

[133] A. Reuss. "Berechnung der Fließgrenze von Mischkristallen auf Grund der Plastizitätsbedingung für Einkristalle ." In: *ZAMM - Zeitschrift für Angewandte Mathematik und Mechanik* 9.1 (1929), pp. 49–58. DOI: 10.1002/zamm.19290090104. URL: https://doi.org/10.1002/zamm.19290090104.

[134] R Hill. “The Elastic Behaviour of a Crystalline Aggregate”. In: *Proceedings of the Physical Society. Section A* 65.5 (May 1952), pp. 349–354. DOI: 10.1088/0370-1298/65/5/307. URL: https://doi.org/10.1088/0370-1298/65/5/307.

[135] Félix Mouhat and François-Xavier Coudert. “Necessary and sufficient elastic stability conditions in various crystal systems”. In: *Physical Review B* 90.22 (Dec. 2014). DOI: 10.1103/physrevb.90.224104. URL: https://doi.org/10.1103/physrevb.90.224104.

[136] Andrew B. Cairns and Andrew L. Goodwin. “Negative linear compressibility”. In: *Physical Chemistry Chemical Physics* 17.32 (2015), pp. 20449–20465. DOI: 10.1039/c5cp00442j. URL: https://doi.org/10.1039/c5cp00442j.

[137] Ken E Evans. “Auxetic polymers: a new range of materials”. In: *Endeavour* 15.4 (Jan. 1991), pp. 170–174. DOI: 10.1016/0160-9327(91)90123-s. URL: https://doi.org/10.1016/0160-9327(91)90123-s.

[138] M. Siddorn, F.-X. Coudert, K. E. Evans, and A. Marmier. “A systematic typology for negative Poisson’s ratio materials and the prediction of complete auxeticity in pure silica zeolite JST”. In: *Physical Chemistry Chemical Physics* 17.27 (2015), pp. 17927–17933. DOI: 10.1039/c5cp01168j. URL: https://doi.org/10.1039/c5cp01168j.

[139] Aurélie U. Ortiz, Anne Boutin, Alain H. Fuchs, and François-Xavier Coudert. “Anisotropic Elastic Properties of Flexible Metal-Organic Frameworks: How Soft are Soft Porous Crystals?” In: *Physical Review Letters* 109.19 (Nov. 2012). DOI: 10.1103/physrevlett.109.195502. URL: https://doi.org/10.1103/physrevlett.109.195502.

[140] Artem R. Oganov and Colin W. Glass. “Crystal structure prediction usingab initioevolutionary techniques: Principles and applications”. In: *The Journal of Chemical Physics* 124.24 (June 2006), p. 244704. DOI: 10.1063/1.2210932. URL: https://doi.org/10.1063/1.2210932.

[141] Artem R. Oganov, Andriy O. Lyakhov, and Mario Valle. “How Evolutionary Crystal Structure Prediction Works—and Why”. In: *Accounts of Chemical Research* 44.3 (Mar. 2011), pp. 227–237. DOI: 10.1021/ar1001318. URL: https://doi.org/10.1021/ar1001318.

[142] Silvia Bahmann and Jens Kortus. “EVO—Evolutionary algorithm for crystal structure prediction”. In: *Computer Physics Communications* 184.6 (June 2013), pp. 1618–1625. DOI: 10.1016/j.cpc.2013.02.007. URL: https://doi.org/10.1016/j.cpc.2013.02.007.

[143] David C. Lonie and Eva Zurek. “XtalOpt: An open-source evolutionary algorithm for crystal structure prediction”. In: *Computer Physics Communications* 182.2 (Feb. 2011), pp. 372–387. DOI: 10.1016/j.cpc.2010.07.048. URL: https://doi.org/10.1016/j.cpc.2010.07.048.

[144] Kevin Ryan, Jeff Lengyel, and Michael Shatruk. “Crystal Structure Prediction via Deep Learning”. In: *Journal of the American Chemical Society* 140.32 (June 2018), pp. 10158–10168. DOI: 10.1021/jacs.8b03913. URL: https://doi.org/10.1021/jacs.8b03913.

[145] Christopher C. Fischer, Kevin J. Tibbetts, Dane Morgan, and Gerbrand Ceder. “Predicting crystal structure by merging data mining with quantum mechanics”. In: *Nature Materials* 5.8 (July 2006), pp. 641–646. DOI: 10.1038/nmat1691. URL: https://doi.org/10.1038/nmat1691.

[146] Stefano Curtarolo, Dane Morgan, Kristin Persson, John Rodgers, and Gerbrand Ceder. “Predicting Crystal Structures with Data Mining of Quantum Calculations”. In: *Physical Review Letters* 91.13 (Sept. 2003). DOI: 10.1103/physrevlett.91.135503. URL: https://doi.org/10.1103/physrevlett.91.135503.

[147] Albert M. Lund, Gabriel I. Pagola, Anita M. Orendt, Marta B. Ferraro, and Julio C. Facelli. “Crystal structure prediction from first principles: The crystal structures of glycine”. In: *Chemical Physics Letters* 626 (Apr. 2015), pp. 20–24. DOI: 10.1016/j.cplett.2015.03.015. URL: https://doi.org/10.1016/j.cplett.2015.03.015.

[148] Rachid Stefan Touzani and Manja Krüger. “First Principles Density Functional Theory Prediction of the Crystal Structure and the Elastic Properties of Mo2ZrB2 and Mo2HfB2”. In: *Crystals* 10.10 (Sept. 2020), p. 865. DOI: 10.3390/cryst10100865. URL: https://doi.org/10.3390/cryst10100865.

[149] John Landers, Gennady Yu. Gor, and Alexander V. Neimark. “Density functional theory methods for characterization of porous materials”. In: *Colloids and Surfaces A: Physicochemical and Engineering Aspects* 437 (Nov. 2013), pp. 3–32. DOI: 10.1016/j.colsurfa.2013.01.007. URL: https://doi.org/10.1016/j.colsurfa.2013.01.007.

[150] Kamal Choudhary, Irina Kalish, Ryan Beams, and Francesca Tavazza. “High-throughput Identification and Characterization of Two-dimensional Materials using Density functional theory”. In: *Scientific Reports* 7.1 (July 2017). DOI: 10.1038/s41598-017-05402-0. URL: https://doi.org/10.1038/s41598-017-05402-0.

[151] Jacco van de Streek, Edith Alig, Simon Parsons, and Liana Vella-Zarb. “A jumping crystal predicted with molecular dynamics and analysed with TLS refinement against powder diffraction data”. In: *IUCrJ* 6.1 (Jan. 2019), pp. 136–144. DOI: 10.1107/s205225251801686x. URL: https://doi.org/10.1107/s205225251801686x.

[152] Jiaxi Zhang and Somnath Ghosh. “Molecular dynamics based study and characterization of deformation mechanisms near a crack in a crystalline material”. In: *Journal of the Mechanics and Physics of Solids* 61.8 (Aug.

2013), pp. 1670–1690. DOI: 10.1016/j.jmps.2013.04.004. URL: https://doi.org/10.1016/j.jmps.2013.04.004.

[153] Oral Büyüköztürk, Markus J. Buehler, Denvid Lau, and Chakrapan Tuakta. "Structural solution using molecular dynamics: Fundamentals and a case study of epoxy-silica interface". In: *International Journal of Solids and Structures* 48.14-15 (July 2011), pp. 2131–2140. DOI: 10.1016/j.ijsolstr.2011.03.018. URL: https://doi.org/10.1016/j.ijsolstr.2011.03.018.

[154] P. C. Schmidt. "Melvin Lax: Symmetry principles in Solid state and Molecular Physics, John Wiley and Sons, London 1974, 499 Seiten, Preis: £ 6.80 (Paper) oder £ 10.55 (Cloth)". In: *Berichte der Bunsengesellschaft für physikalische Chemie* 79.12 (Dec. 1975), pp. 1249–1250. DOI: 10.1002/bbpc.19750791215. URL: https://doi.org/10.1002/bbpc.19750791215.

[155] G. Burns and A. Glazer. *Space groups for solid state scientists*. Boston: Academic Press, 1990. ISBN: 9780080964126.

[156] Ulrich Müller. *Symmetry Relationships between Crystal Structures*. Oxford University Press, Apr. 2013. DOI: 10.1093/acprof:oso/9780199669950.001.0001.

[157] John Baez. *Felix Klein's Erlangen Program.* URL: https://math.ucr.edu/home/baez/erlangen/ (visited on 06/29/2021).

[158] Eric W. Weisstein. *"Space-Filling Polyhedron." From MathWorld–A Wolfram Web Resource.* URL: https://mathworld.wolfram.com/Space-FillingPolyhedron.html (visited on 06/27/2021).

[159] S. Torquato and Y. Jiao. "Dense packings of polyhedra: Platonic and Archimedean solids". In: *Physical Review E* 80.4 (Oct. 2009). DOI: 10.1103/physreve.80.041104. URL: https://doi.org/10.1103/physreve.80.041104.

[160] B.N. Delone, Nikolai Dolbilin, M.I. Shtogrin, and R.V. Galiulin. "A local criterion for regularity of a system of points". In: *Soviet Mathematics. Doklady* 17 (Jan. 1976), pp. 19–21.

[161] István Hargittai and Magdolna Hargittai. *Symmetry through the Eyes of a Chemist*. Springer Netherlands, 2009, p. 520. ISBN: 978-1-4020-5627-7. DOI: 10.1007/978-1-4020-5628-4l. URL: https://www.springer.com/gp/book/9781402056277.

[162] H. Bärnighausen. "Group-Subgroup Relations between Space Groups: A Useful Tool in Crystal Chemistry". In: *MATCH Commun. Math. Chem.* 9 (1980), pp. 139–175.

[163] K. J. Köhler. "Subgroup-Relations between Crystallographic Groups". In: *MATCH Commun. Math. Chem.* 9 (1980), pp. 191–207.

[164] Michael E. Levinshtein, Sergey L. Rumyantsev, and Michael S. Shur. "Properties of advanced semiconductor materials : GaN, AlN, InN, BN, SiC, SiGe". In: 2001.

[165] Yutaka Nigara. "Measurement of the Optical Constants of Yttrium Oxide". In: *Jpn. J. Appl. Phys.* 7.4 (Apr. 1968), pp. 404–408. DOI: 10.1143/jjap.7.404. URL: https://doi.org/10.1143%5C%2Fjjap.7.404.

[166] D. L. Wood, Kurt Nassau, T. Y. Kometani, and D. L. Nash. "Optical properties of cubic hafnia stabilized with yttria". In: *Appl. Opt.* 29.4 (Feb. 1990), pp. 604–607. URL: http://ao.osa.org/abstract.cfm?URI=ao-29-4-604.

[167] H.G. Craighead, R. Bartynsky, R.A. Buhrman, L. Wojcik, and A.J. Sievers. "Metal/insulator composite selective absorbers". In: *Solar Energy Materials* 1.1-2 (Feb. 1979), pp. 105–124. DOI: 10.1016/0165-1633(79)90061-3. URL: https://doi.org/10.1016/0165-1633(79)90061-3.

SISUKOKKUVÕTE (SUMMARY IN ESTONIAN)

Haruldaste muldmetallide hüdriididel rajanevate nutimaterjalide esmaste printsiipide uuringud

Käesoleva doktoritöö peamine eesmärk oli uurida haruldaste muldmetallide oksühüdriide Y-H-O, La-H-O, Gd-H-O, kombineerides teoreetilisi ja arvutuslikke meetodeid.

Rühmateooria meetodite, mitmikanioonkeemilise argumentatsiooni ja tihedusfunktsionaalteooria arvutuste kombinatsiooni abil oleme tuvastanud ja kirjeldanud kõige tõenäolisemaid struktuurilisi ja koostislikke konfiguratsioone haruldaste muldmetallide oksühüdriidide süsteemides. Lähtudes suurest hulgast prognoositud erinevate kristallstruktuuridega ja hapniku/vesiniku osakaaludega ühenditest, töötasime esimestena välja ternaarse faasidiagrammi Y-H-O koostiste tarvis. See võimaldas meil kirjeldada hapniku kui ternaarühendite mitmikaniooniliste raamstruktuuride peamise stabiliseerija võtmerolli kristallilistes oksühüdriidides.

Oleme näidanud, et teatud juhtudel peaksid oksühüdriidiühendi kondenseerumisel toimuma katioonide ja anioonide ekstsentrilised nihked, et tagada stabiilne struktuur. See mõju võib tingida kristallstruktuuri inversioonisümmeetria rikkumise ja põhjustada laengutiheduse makroskoopilise asümmeetria. Kõikide kolmekomponentsete oksühüdriidide koostiste hulgast leidsime, et Ln_2H_4O (Ln = Y, La) võib stabiliseeruda kolmes mittetsentrosümmeetrilises faasis, millel on monokliinne, ortorombiline ja trigonaalne struktuur. Meie prognoosid näitasid, et Ln_2H_4O monokliinsed ja ortorombilised polaarsed faasid ilmutavad erakordset piesoelektrilist vastust ja võivad tagada ka kõrge elektromehaanilise jõudluse.

Oleme näidanud, et hapniku aatomite spetsiifiline integreerimine ütriumoksühüdriidi süsteemis võib viia uue klassi anorgaaniliste kristalliliste materjalide - metallhüdroksühüdriidide, mille keemiline koostis on $M_2H_3O(OH)$ (M = Y, Sc, La ja Gd) – tekkimiseni. Leiti, et hapniku poolt põhjustatud spetsiifilised kristallstruktuuri muutused põhjustavad mõnede vesinikuioonide laengu muutumise negatiivsest H^-ist positiivseks H^+-iks, moodustades seega hüdroksüülgruppides prootonite asukohti. Laengu tugev lokaliseerumine vesiniku positsioonidel, mis on tingitud erilisest aatomikorrastusest, on oluline tegur, mis stabiliseerib metallkatioonide ja -anioonide kiraalset struktuurilist paigutust, moodustades spiraalseid kõveraid $M_2H_3O(OH)$ tetragonaalses struktuuris. Täpsete DFT-arvutuste tulemused on näidanud, et seda täielikult kiraalse struktuuriga materjali saab kasutada mittelineaarses optikas paljutõotavate rakenduste kavandamiseks ja arendamiseks.

Polaarses oksühüdriidsüsteemis Ln_2H_4O toimunud asendusefektide uurimise põhjal ennustasime uue mitme aniooniga materjalide perekonda – $Ln_2OF_{2-x}Cl_xH_2$ (Ln = Y, La, Gd) –, milles unikaalsed elastsed omadused on ühendatud erakordsete piesoelektriliste omadustega. See avab tee täiustatud energiakogumisseadmete väljatöötamisele, mis võiksid ühendada ühelt poolt piesoelektriliste polümeeride, nagu PVDF, kõrge piesoelektrilise võimsuse ja elastse pehmuse ning teiselt poolt

tahke piesoelektrilise keraamika termilise ja kõrge mehaanilise stabiilsuse. Meie hinnangud energia kogumise efektiivsuse kohta näitasid, et piesoelektrilise energia kogumise seadme väljundvõimsus võib Ln_2OClFH_2 süsteemi kasutamise korral olla umbes 5-10 korda suurem kui kaubanduslikult pakutava PZT-5H keraamika puhul ja umbes 3-4 korda suurem kui kaubanduslikult pakutavate piesoelektriliste polümeeride puhul.

Et näidata, kuidas kasutada valguse refraktsiooni, läbivuse ja peegelduse koosmõju koos valguslainete siseinterferentsmõjuga, pakkusime välja kaks erinevat optiliste katete prototüüpi, milles õhukesed oksühüdriidist kiled täidavad võtmerolli. (i) Väikese emissiooniga katte mudel, mis peaks blokeerima ultraviolettkiirgust ja teatud määral ka päikese infrapunakiirguse põhjustatud kuumust. Mudeli efektiivsus seisneb selles, et nähtav valgusvoog võib levida kõrge läbivusastmega (üle 90%) ja madala peegeldumisastmega (alla 10%). (ii) Valgust neelava mittepeegeldava katte mudel, mis peaks näitama kõrget valguse neeldumist ja madalat valguspeegeldust. Simulatsioonitulemused on näidanud, et esitatud mudel võib olla peamiseks komponendiks lairibaneeldumiskattes. Tavalise langusnurga korral võib süsteem neelata umbes 99.7% valgusest laias lainepikkuste vahemikus 375-550 nm; suurim neelduvus, 99.98%, saavutatakse 395 nm puhul.

Sümmeetriapõhiste meetodite rakendamine koos täpsete DFT-arvutustega on võimaldanud prognoosida ja iseloomustada erineva keemilise koostise ja struktuuriga materjale. Meie lähenemise põhipunkt on see, et kolmemõõtmelise kristallsüsteemi võregeomeetria modelleerimine ei nõua eksperimentaalseid teadmisi aatomite ruumilise paigutuse kohta tavastruktuuris. Konkreetse struktuuri evolutsiooni modelleerimisel võrreldakse hierarhias lubatud allstruktuuride erinevaid kristalliseerumisteid energia- ja stabiilsustingimuste suhtes.

ACKNOWLEDGEMENTS

I would like to express my deep sense of gratitude to my supervisors Dr. Aleksandr Pishtshev and Prof. Dr. Smagul Karazhanov for their all-round support, starting from help with research, publishing articles and writing the dissertation to giving advice on the everyday hardships of a PhD student. I would like to thank all the co-authors for their contribution to the publications.

None of my scientific work would have been possible without the continuous support of my wife, Arina.

The research was financed by the European Union through the European Regional Development Fund, Smart specialization doctoral stipend funded by the European Regional Development Fund and the Republic of Estonia, as well as Kristjan Jaak Scholarship and Dora Plus PhD student mobility grants for short study visits and participation in the conferences.

PUBLICATIONS

CURRICULUM VITAE

Personal data

Name: Evgenii Strugovshchikov
Date of birth: 17.10.1991
Phone: +37256773156
E-mail: evgenii.strugovshchikov@ut.ee

Education

2011–2017 NRNU "Moscow Engineering Physics Institute" (MEPhI), Specialist's Degree in Materials science

2017–2021 University of Tartu, Doctor of Philosophy, Materials Science

Employment

2016–2017 ONIL 709, NRNU "Moscow Engineering Physics Institute" (MEPhI), Engineer

List of publications

[I] Aleksandr Pishtshev, **Evgenii Strugovshchikov**, and Smagul Karazhanov. "Conceptual Design of Yttrium Oxyhydrides: Phase Diagram, Structure, and Properties". In: *Cryst. Growth Des.* 19.5 (2019), pp. 2574–2582. DOI: https://doi.org/10.1021/acs.cgd.8b01596.

[II] Aleksandr Pishtshev and **Evgenii Strugovshchikov**. "Computational prediction of Ferro- and Piezoelectricity in Lead-free Oxyhydrides Ln_2H_4O (Ln = Y, La)". In: *Adv. Theory Simul.* 2.12 (2019), p. 1900144. DOI: https://doi.org/10.1002/adts.201900144.

[III] Aleksandr Pishtshev, **Evgenii Strugovshchikov**, and Smagul Karazhanov. "On prediction of a novel chiral material $Y_2H_3O(OH)$: A hydroxyhydride holding hydridic and protonic hydrogens". In: *Materials* 13.4 (2020), p. 994. DOI: https://doi.org/10.3390/ma13040994.

[IV] Elbruz Murat Baba, Jose Montero, **Evgenii Strugovshchikov**, Esra Özkan Zayim, and Smagul Karazhanov. "Light-induced breathing in photochromic yttrium oxyhydrides". In: *Phys. Rev. Mater.* 4.2 (2020), p. 025201. DOI: https://doi.org/10.1103/PhysRevMaterials.4.025201.

[V] **Evgenii Strugovshchikov** and Aleksandr Pishtshev. "Exploring The Anion Chemical Space of $Ln_2OF_{2-x}Cl_xH_2$ (Ln=Y,La,Gd): A Model of Electroelastic Material with High Mechanical Sensitivity and Energy Harvesting". In: *Mater. Horiz* 8.2 (2021), pp. 577–588. DOI: https://doi.org/10.1039/D0MH01524E.

[VI] **Evgenii Strugovshchikov**, Aleksandr Pishtshev, and Smagul Karazhanov. "Orthogonal chemistry in the design of rare-earth metal oxyhydrides". In: *Pure Appl. Chem.* -.- (2021), pp. -. DOI: https://doi.org/10.1515/pac-2021-0207.

[VII] **Evgenii Strugovshchikov**, Aleksandr Pishtshev, and Smagul Karazhanov. "Theoretical design of effective multilayer optical coatings using oxyhydride thin films". In: *Phys. Status Solidi B* -.- (2021), pp. -. DOI: https://doi.org/10.1002/pssb.202100179.

[VIII] P. V. Borisyuk, E. V. Chubunova, Yu. Yu. Lebedinskii, E. V. Tkalya, O. S. Vasilyev, V. P. Yakovlev, **E. Strugovshchikov**, D. Mamedov, A. Pishtshev, and S. Zh. Karazhanov. "Experimental studies of thorium ion implantation from pulse laser plasma into thin silicon oxide layers". In: *Laser Physics Letters* 15.5 (2018), p. 056101. DOI: https://doi.org/10.1088/1612-202x/aaacf8.

[IX] E.A. Vagapova, **E. Strugovshchikov**, E.O. Orlovskaya, A.S. Vanetsev, L. Dolgov, L. Puust, L.D. Iskhakova, U. Maeorg, A. Pishtshev, and Yu.V. Orlovskii. "Combined spectroscopic and DFT studies of local defect structures in beta-tricalcium phosphate doped with Nd(III)". In: *Journal of Alloys and Compounds* 15.5 (2021), p. 160305. DOI: https://doi.org/10.1016/j.jallcom.2021.160305.

6 oral and 2 poster presentations at international conferences

Media reporting

[X] "New, exotic materials: Getting oxygen into yttrium hydrides". In: *Research Outreach* 122 (May 2021). DOI: 10.32907/ro-122-1291164836. URL: https://doi.org/10.32907/ro-122-1291164836.

ELULOOKIRJELDUS

Isikuandmed

Nimi: Evgenii Strugovshchikov
Sünniaeg: 17.10.1991
Telefon: +37256773156
E-post: evgenii.strugovshchikov@ut.ee

Haridus

2011–2017 NRNU "Moscow Engineering Physics Institute" (MEPhI), Materjaliteaduse spetsialist
2017–2021 Tartu Ülikool, doktoriõpe, materjaliteadus

Teenistuskäik

2016–2017 ONIL 709, NRNU "Moscow Engineering Physics Institute" (MEPhI), Insener

Publikatsioonide loetelu

[I] Aleksandr Pishtshev, **Evgenii Strugovshchikov** ja Smagul Karazhanov. "Conceptual Design of Yttrium Oxyhydrides: Phase Diagram, Structure, and Properties". *Cryst. Growth Des.* 19.5 (2019), lk. 2574–2582. DOI: https://doi.org/10.1021/acs.cgd.8b01596.

[II] Aleksandr Pishtshev ja **Evgenii Strugovshchikov**. "Computational prediction of Ferro- and Piezoelectricity in Lead-free Oxyhydrides Ln_2H_4O (Ln = Y, La)". *Adv. Theory Simul.* 2.12 (2019), lk. 1900144. DOI: https://doi.org/10.1002/adts.201900144.

[III] Aleksandr Pishtshev, **Evgenii Strugovshchikov** ja Smagul Karazhanov. "On prediction of a novel chiral material $Y_2H_3O(OH)$: A hydroxyhydride holding hydridic and protonic hydrogens". *Materials* 13.4 (2020), lk. 994. DOI: https://doi.org/10.3390/ma13040994.

[IV] Elbruz Murat Baba, Jose Montero, **Evgenii Strugovshchikov**, Esra Özkan Zayim ja Smagul Karazhanov. "Light-induced breathing in photochromic yttrium oxyhydrides". *Phys. Rev. Mater.* 4.2 (2020), lk. 025201. DOI: https://doi.org/10.1103/PhysRevMaterials.4.025201.

[V] **Evgenii Strugovshchikov** ja Aleksandr Pishtshev. "Exploring The Anion Chemical Space of $Ln_2OF_{2-x}Cl_xH_2$ (Ln=Y,La,Gd): A Model of Electroelastic Material with High Mechanical Sensitivity and Energy Harvesting". *Mater. Horiz* 8.2 (2021), lk. 577–588. DOI: https://doi.org/10.1039/D0MH01524E.

[VI] **Evgenii Strugovshchikov**, Aleksandr Pishtshev ja Smagul Karazhanov. "Orthogonal chemistry in the design of rare-earth metal oxyhydrides". *Pure Appl. Chem.* -.- (2021), lk. -. DOI: https://doi.org/10.1515/pac-2021-0207.

[VII] **Evgenii Strugovshchikov**, Aleksandr Pishtshev ja Smagul Karazhanov. "Theoretical design of effective multilayer optical coatings using oxyhydride thin films". *Phys. Status Solidi B* -.- (2021), lk. -. DOI: https://doi.org/10.1002/pssb.202100179.

[VIII] P. V. Borisyuk, E. V. Chubunova, Yu. Yu. Lebedinskii, E. V. Tkalya, O. S. Vasilyev, V. P. Yakovlev, **E. Strugovshchikov**, D. Mamedov, A. Pishtshev ja S. Zh. Karazhanov. "Experimental studies of thorium ion implantation from pulse laser plasma into thin silicon oxide layers". *Laser Physics Letters* 15.5 (2018), lk. 056101. DOI: https://doi.org/10.1088/1612-202x/aaacf8.

[IX] E.A. Vagapova, **E. Strugovshchikov**, E.O. Orlovskaya, A.S. Vanetsev, L. Dolgov, L. Puust, L.D. Iskhakova, U. Maeorg, A. Pishtshev ja Yu.V. Orlovskii. "Combined spectroscopic and DFT studies of local defect structures in beta-tricalcium phosphate doped with Nd(III)". *Journal of Alloys and Compounds* 15.5 (2021), lk. 160305. DOI: https://doi.org/10.1016/j.jallcom.2021.160305.

6 suulist ja 2 stendiettekannet rahvusvahelistel konverentsidel

Meediakajastus

[X] "New, exotic materials: Getting oxygen into yttrium hydrides". *Research Outreach* 122 (mai 2021). DOI: 10.32907/ro-122-1291164836. URL: https://doi.org/10.32907/ro-122-1291164836.

DISSERTATIONES SCIENTIAE MATERIALIS UNIVERSITATIS TARTUENSIS

1. **Martin Järvekülg**. Tubular microstructures by Hf-, Zr- and Ti-butoxide gel sheet rolling. Tartu, 2011, 112 p.
2. **Sergei Vlassov.** Investigation of nanoscale interactions and mechanical properties of nanostructures using quartz tuning fork based real-time measurements. Tartu, 2011, 171 p.
3. **Margus Kodu**. Pulsed Laser Deposition of Magnesium Oxide and Barium Ternary Oxides for Plasma Display Protective Layers. Tartu, 2011, 89 p.
4. **Rainer Pärna**. Surface studies of some oxide films. Tartu, 2011, 129 p.
5. **Jevgeni Šulga**. Self-assembly and interaction of nanostructures. Tartu, 2011, 114 p.
6. **Wojciech Kuznik**. Quantum-chemical computer simulations of the linear and non-linear optical properties of pyrazoloquinoline and dicyanopyrazine derivatives. Tartu, 2012, 89 p.
7. **Leonid Dorogin**. Structural and tribological properties of zero- and one-dimensional nanocrystals. Tartu, 2012, 193 p.
8. **Viljar Palmre**. Fabrication and characterization of microporous carbon-based electroactive polymer actuators. Tartu, 2012, 99 p.
9. **Madis Paalo**. Synthesis of CNT-metal oxide nanocomposites: sol-gel process, rheology, structural and functional properties. Tartu, 2014, 175 p.
10. **Raul Välbe**. Developement of ionic liquid composites by sol-gel method for elaboration of industrial nano- and microstructures. Tartu, 2014, 97 p.
11. **Urmas Joost**. Impurity and preparation dependent properties of titania thin films. Tartu, 2014, 155 p.
12. **Madis Umalas**. Application of sol-gel technology for production of ceramic nanocomposites and functional coatings. Tartu, 2015, 136 p.
13. **Elena Samsonova**. Energy transfer probe as a tool to study morphological and structural origins of fluorescence quenching in rare-earth doped nanophosphors. Tartu, 2015, 114 p.
14. **Jay Mondal**. Novel Corrosion Protective Nanostructured Composite Coatings. Tartu, 2016, 104 p.
15. **Kathriin Utt**. Metal oxide mesostructures for optical applications. Tartu, 2016, 88 p.
16. **Kaido Siimon**. Electrospun gelatin cross-linked by glucose. Tartu, 2016, 84 p.
17. **Marko Part**. Combined three-dimensional sol-gel structures and atomic layer deposited thin films. Tartu, 2017, 162 p.
18. **Pejman Rasti**. Analysis of Remote Sensing Image Super Resolution using Fluid Lenses. Tartu, 2017, 188 p.
19. **Ivo Romet**. Recombination luminescence of doped borates: origin and application prospects in dosimetry. Tartu, 2017, 111 p.

20. **Vladimir I. Kondratiev**. Processing and characterization of transparent electrode materials. Tartu, 2017, 111 p.
21. **Taivo Jõgiaas**. Mechanical properties of atomic layer deposited thin films and nanocomposites. Tartu, 2017, 125 p.
22. **Lauri Aarik**. Atomic layer deposition and characterization of thin oxide films for application in protective coatings. Tartu, 2017, 180 p.
23. **Triin Kangur**. Preparation and functional properties of stochastic micro-structured sol-gel silica materials. Tartu, 2018, 96 p.
24. **Marta Berholts**. Fragmentation of ionic and hydrogen-bonded molecules induced by synchrotron radiation. Tartu, 2018, 126 p.
25. **Priit Priimägi**. Development and optimization of 3D-microbatteries. Tartu, 2018, 118 p.
26. **Siim Hödemann**. Residual stress determination in chemically strengthened and thermally tempered glass plates using scattered light method. Tartu, 2019, 146 p.
27. **Jekaterina Kozlova**. Complex characterization of graphene structures on nanometer level. Tartu, 2019, 206 p.
28. **Kristjan Kalam**. Magnetic, electric and structural properties of atomic layer deposited zirconia-based nanolaminates and mixtures. Tartu, 2020, 94 p.
29. **Triinu Vihmann**. Ionic liquids: synthesis and application in lubrication and lithography. Tartu, 2020, 102 p.
30. **Helina Seemen**. Atomic layer deposition and microscopic analysis of magnetically and electrically polarizable thin solid films. Tartu, 2021, 126 p.
31. **Ekaterina Vagapova.** Fluorescence quenching in inorganic crystalline solids activated by neodymium ions; from bulk to micro- and nanocrystals. Tartu, 2021, 116 p.